Title: Pathogenic IgE-fated memory B cell responses retain functional plasticity

Authors: Kelly Bruton,[1†‡*], Allyssa Phelps,[1‡] Atai Ariaz[1], Allison Fang[1], Tina D. Walker[1], Jianping Wen[1], Sharon S. Khavkine-Binstock[1], Danielle Della Libera[1], Olivia Mann-Delany[1], Niels Peter H. Knudsen[2], Siyon Gadkar[1], Emily Grydziuszko[1], Joshua F. E. Koenig[1], Aidan Gagnon[1], Susan Waserman[1], Peter S. Andersen[2], Manel Jordana[1]

Affiliations:

[1]Schroeder Allergy & Immunology Research Institute and Department of Medicine (Division of Clinical Immunology & Allergy), McMaster University; Hamilton, Ontario, CA.

[2]ALK-Abelló A/S; Hørsholm, DK

[†]Current Address: Department of Pathology, Stanford University School of Medicine; Stanford, California, USA.

[‡]These authors contributed equally to this work.

*Corresponding author. Email: brutonk@stanford.edu

Abstract: Long-lived immunoglobulin (Ig) E responses against innocuous environmental and dietary antigens (Ags) are maintained by an IgG1-dominant memory B cell (MBC) compartment primed for IL-4 responsiveness. The plasticity of the MBC compartment destined for IgE class switch recombination (CSR), however, remains poorly understood. In this work, we report a critical IL-4/IL-13 dependency for the pathogenic IgE fate of type 2-polarized MBCs. Initiating a recall response in the absence of IL-4/IL-13 signaling diminished the type 2 MBC phenotype in mice and humans and, in mice, permitted the emergence of long-lived Ag-specific IgG2c^{+}

MBCs. The divergence to a type 1-like response was dependent on IFN-γ signaling and arose from both unswitched and class-switched Ag-specific B cells *in vivo*. This reprogrammed fate was sustained even beyond therapeutic intervention, revealing fundamental insight into the plasticity of the allergen-specific MBC response.

One Sentence Summary: B cell responses to allergens can be reprogrammed away from a pathogenic fate through IL-4/IL-13 signaling blockade.

Main Text:

INTRODUCTION

Classical immunological memory is marked by the propensity for rapid and optimized responses upon re-exposure to the target antigen (Ag). Within the B cell compartment, immunological memory is distinguished by high-affinity binding to Ag, a class-switched constant region conferring specialized effector functions, and altered cellular processes (*e.g.,* metabolism). Following vaccination, for example, viral exposure rapidly reactivates memory B cells (MBCs) facilitating plasma cell differentiation and boosting of neutralizing IgG titers, lessening the opportunity for infection (*1–3*). MBC reactivation, however, is pathogenic when perpetuating inflammatory responses to innocuous Ag, as occurs in allergic disease.

Allergies categorized as type I hypersensitivities are mediated by IgE. Humoral IgE responses are relatively short-lasting, yet reactivity to some allergens (*e.g.,* peanuts) can persist for a lifetime (*4–8*). Central to this persistence are IgG1^{+} MBCs which undergo sequential class-switching to replenish the transient IgE plasma cell pool (*5*, *9–12*). Likewise, it has been identified that IgE-fated MBCs, termed MBC2s, exhibit an IL-4-responsive phenotype marked by high expression of CD23 (FcεRII) and IL-4 receptor α (IL-4Rα) and low CD32 (FcγRII)

30 expression (*13–15*). Indeed, seminal work on IgE established IL-4 as a critical molecule for IgE
31 class switch recombination (CSR) upon primary sensitization (*16*, *17*). Despite the formation of a
32 more specialized MBC compartment, IL-4 continues to be required for secondary IgE responses
33 (*18–20*). Beyond inhibition of IgE CSR, loss of IL-4 signaling upregulates IFN-γ production
34 suggestive of plasticity within the T cell compartment (*18*). Whether a parallel degree of
35 plasticity exists in the Ag-specific MBC compartment, or if the commitment is irreversible,
36 remains to be elucidated.

37 In this study, we identified a previously unrecognized plasticity of the MBC response within type
38 2 immunity. By inhibiting IL-4 signaling in a recall response, the pathogenic MBC2 phenotype
39 was diminished, and upregulation of IFN-γ supported the emergence of long-lived IgG2c
40 responses. Even beyond transient IL-4Rα blockade, IgG2c reemerged upon Ag exposure,
41 suggesting some degree of stability in the type I-like reprogrammed antibody (Ab) response
42 despite discontinued IL-4Rα blockade. Ag-specific IgG2b/c responses appeared to derive from
43 both unswitched B cells and class-switched MBCs, where the addition of a type 1 adjuvant could
44 augment the redirection of IgG1 memory to IgG2b/c. Collectively, our findings elucidate a
45 malleable fate of the pathogenic IgE-fated MBC response and highlights the potential to
46 therapeutically reprogram refractory lifelong allergies.

47 **RESULTS**

48 **IL-4Rα signaling augments secondary germinal center activity**

49 To assess the impact of *in vivo* IL-4Rα blockade (A4RA) on the B cell compartment in type 2
50 immunity, we employed a well characterized model of epicutaneous sensitization to ovalbumin
51 (OVA). This strategy establishes a humoral OVA-IgG1 response and IgG1^{+} MBCs which, upon

52 subsequent non-sensitizing subcutaneous (s.c.) re-exposures, facilitate IgE production and IgE-
53 mediated clinical reactivity (*21*). With temporal control over the IgE response, we treated
54 sensitized mice with A4RA or an isotype control (IC) prior to s.c. re-exposures, as previously
55 described (*18*). Draining lymph nodes (dLNs) and spleens were collected for single-cell RNA-
56 sequencing (scRNA-seq), single-cell VDJ-sequencing (scVDJ-seq), and flow cytometry, and
57 blood was collected for immunoglobulin (Ig) analysis (**Fig. 1A**). For scRNA- and scVDJ-seq
58 experiments an additional group of mice were administered cholera toxin (CT) and OVA (s.c.) to
59 model a classical type 2 immunization strategy that yields robust humoral IgE responses and
60 IgG1^{+} MBCs.

61 Four weeks following immunization and s.c. re-exposures, paired scRNA-seq and scVDJ-seq
62 were performed on 7,369 B cells. Clustering analysis revealed subsets of naïve B cells (*Ighm*$^{+}$
63 *Ighd*$^{+}$), class-switched MBCs (*Ighm*$^{-}$ *Ighd*$^{-}$), and an *Ighd*$^{+/-}$ subset defined by high *Fcrl5* and
64 *Apoe* expression (**Fig. 1B and 1C**). Naïve-1 was the dominant naïve subset in CT and IC-treated
65 mice, though was almost completely replaced by the Naïve-4 cluster in A4RA-treated mice (**Fig.**
66 **1D**). Relative to other B cell clusters, Naïve-4 cells exhibited marked transcriptional
67 downregulation, particularly across several metabolic pathways and genes relating to Ag
68 presentation and cellular localization (**fig. S1A and S1B**). Indeed, it has been shown that *in vitro*
69 B cell stimulation with IL-4 initiates metabolic reprogramming and MHC-II upregulation (*22–*
70 *24*). The Naïve-3 subset, which was almost exclusively found in epicutaneously sensitized mice,
71 had upregulated *Il31ra* expression, the ligand (IL-31) of which is implicated in promoting
72 dermatitis (**fig. S1C and S1D**) (*25*). Other naïve and MBC clusters were similarly represented
73 between the three groups. Across all core naïve clusters (1-5) and MBCs, A4RA treatment

74 resulted in downregulated oxidative phosphorylation and B cell receptor (BCR) signaling gene
75 modules – two imperative processes for germinal center (GC) activity (**Fig. 1E**) (*26*, *27*).

76 Previous reports have demonstrated a critical requirement of IL-4 signaling for primary GC
77 activity in models of type 2 immunity, though it remains unclear whether this requirement is
78 maintained for secondary responses where primary responses can prime MBCs for a GC or PC
79 fate (*28–30*). The requirement of secondary T follicular helper cell-mediated B cell activation to
80 mount an IgE response in epicutaneously sensitized mice was confirmed using CD40L blockade
81 before and during s.c. re-exposures, whereby anti-CD40L prevented OVA-specific IgE
82 production and clinical reactivity (**fig. S2A-C**). To investigate how an IL-4/IL-13 signaling
83 deficiency might impact secondary GCs, we utilized the paired scRNA- and scVDJ-seq data to
84 determine the extent of somatic hypermutation (SHM) within the MBC cluster. Despite an
85 absence of highly mutated sequences with A4RA treatment, the overall extent of SHM was not
86 significantly different between groups (**Fig. 1F**).

87 As the above findings provided only transcriptional insight within the bulk (non-Ag-specific) B
88 cell repertoire, we assessed the impact of A4RA on OVA-specific B cells by flow cytometry
89 using fluorochrome-conjugated OVA tetramers (*31*, *32*). In agreement with the altered B cell
90 metabolic profile in the transcriptomic data suggestive of compromised B cell survival and/or
91 proliferative capacity, the frequency of OVA^+ B cells was 3-fold lower in A4RA-treated mice,
92 with an average of 406 versus 1269 cells per dLN pair in A4RA and IC groups, respectively
93 (**Fig. 1G and 1H**). Expression of CD38 and GL7 identifies three populations of B cells differing
94 in their activation states: $CD38^+$ $GL7^-$ resting naïve/memory (1), $CD38^+$ $GL7^+$ transitional or
95 multipotent precursor cells (2), and $CD38^-$ $GL7^+$ GC B cells (3) (**Fig. 1I**) (*33*). At three days
96 post-re-exposures, the A4RA group had significantly impaired OVA-specific B cell activation,

97 evidenced by an increased frequency of $CD38^+$ $GL7^-$ OVA-specific B cells and a concomitant
98 decrease in the $CD38^-$ $GL7^+$ population (**Fig. 1J**). However, 23% of OVA-specific B cells in
99 A4RA-treated mice were in a transitional state compared to 2.6% in IC-treated mice, which
100 suggested that loss of IL-4/IL-13 signaling altered the kinetics of MBC reactivation. Indeed,
101 assessment of GC activity at 7-, 14-, and 28-days post-re-exposure demonstrated that the
102 proportion of OVA^+ B cells that ultimately participate in GCs is no different between groups and
103 A4RA treatment merely stalls early GC formation (**Fig. 1K**). Taken together, these data suggest
104 that loss of IL-4/IL-13 signaling elicits profound transcriptional changes to naïve B cells and
105 MBCs, but GC-dependent recall responses can ultimately proceed.

106 **MBC2 phenotype is diminished with IL-4Rα blockade in mice and humans**

107 MBC2s have been identified as an important reservoir for pathological IgE responses (*14*, *15*).
108 Previously, IL-4 was shown to be necessary for MBC2 development and, likewise, blockade of
109 IL-4/IL-13 signaling issued a decline in MBC2 frequency (*13*, *14*, *18*). Despite the observed
110 decrease in MBC2s a small number persist, though whether expression of the pathogenic IL-4-
111 responsive phenotype is maintained to the same extent has not been explored.

112 To address this, we leveraged publicly reposited B cell scRNA-seq datasets involving
113 perturbation of IL-4/IL-13 signaling. Including our own data generated above, our analysis
114 involved four datasets comprising both mouse and human, various models of type 2 immunity,
115 enhanced and abrogated IL-4/IL-13 signaling, and with or without Ag re-exposure (**Fig. 2A**) (*18*,
116 *34*, *35*). For each dataset, unsupervised clustering was performed on B cells (*Cd79a*$^+$), which
117 resolved clusters of MBCs classified by absence of *Ighd*, *Tcl1a* (human), and *Bcl6* (mouse) and
118 the presence of *Hhex* (mouse) and *Ccr6* (mouse) expression (**Fig. 2B and S3A-D**). *Fcer2*, *Il4r*,
119 and *Ighg1* expression was compared between each control and interventional group to evaluate

120 the impact of enhanced or inhibited IL-4/IL-13 signaling on MBC2-related gene expression (**Fig.**
121 **2C**). *Fcer2* expression in MBCs was consistently downregulated across datasets involving IL-
122 4/IL-13 signaling inhibition. IL-4Rα blockade also elicited a decline in *Il4r* expression, apart
123 from epicutaneously sensitized mice where *Il4r* transcript abundance was also low in IC mice.
124 Conversely, with increased IL-4/IL-13 bioavailability to B cells through elimination of its uptake
125 by lymphoid stromal cells (*Ccl19*$^{Cre/+}$ *Il4ra*$^{fl/fl}$ bone marrow chimeras; LSC Il4r deficiency),
126 *Fcer2* and *Il4r* expression was enhanced within the MBC cluster (*34*). Intriguingly, *Ighg1*
127 expression was downregulated only in experimental systems involving Ag re-exposure during
128 IL-4Rα blockade.

129 To corroborate the diminished MBC2 phenotype within Ag-specific cells, we assessed co-
130 expression of surface IL-4Rα and CD23 on tetramer^{+} MBCs by flow cytometry four weeks
131 following *s.c.* re-exposures in epicutaneously sensitized mice (**Fig. 2D**). A4RA-treated mice
132 exhibited a 61% reduction in the frequency of IL-4Rα^{+} CD23^{+} cells in the OVA-specific MBC
133 compartment (**Fig. 2E**). IL-4Rα did not appear to be maintained on the cell surface bound to
134 A4RA, as surface rat-IgG2a (A4RA Fc region) was undetectable at this timepoint (**fig. S4**).
135 Consistent with a role of IL-4 in inducing CD23 expression, A4RA treatment decreased surface
136 expression of CD23, even amongst IL-4R^{low} cells (**Fig. 2F**) (*36*). CD23 downregulation was not,
137 however, unique to Ag-specific cells, but instead was broadly observed throughout non-specific
138 MBCs (**Fig. 2F**).

139 To also validate the human scRNA-seq observations, we stimulated peripheral blood
140 mononuclear cells (PBMCs) from peanut-allergic donors (n=3) with crude peanut extract for
141 eight days in the presence or absence of A4RA. We have previously shown that 8% of MBCs in
142 unstimulated cultures exhibit an MBC2-like transcriptional profile and expand to over 20% upon

143 peanut stimulation. Extending upon this to elucidate how A4RA treatment impacted protein
144 expression of MBC2 markers, we could observe CD23$^+$ IL-4Rα$^+$ class-switched B cells in
145 stimulated cells but these were virtually undetectable with A4RA treatment (**Fig. 2G**). Consistent
146 with previous reports, CD23$^+$ IL-4Rα$^+$ cells had variable CD27 expression, though we found that
147 both populations were similarly impacted by A4RA (**Fig. 2H**) (*13*, *14*). Moreover, as was
148 observed in mice, A4RA broadly decreased CD23 mean fluorescence intensity (MFI) within
149 class-switched B cells (**Fig. 2I**). Collectively, these data demonstrate a conserved requirement
150 for IL-4/IL-13 signaling to maintain heightened type 2 polarization within established MBC
151 compartments, which contests a previous suggestion regarding MBC2 phenotypic resiliency
152 (*13*). These data also raise the issue of how Ag re-exposure during IL-4Rα blockade may skew
153 the isotype distribution away from IgG1 – the dominant intermediary for IgE CSR.

154 We acknowledge that, despite using different Ab clones for IL-4Rα blockade and detection by
155 flow cytometry, it is possible that steric hindrance may have diminished the detection of surface
156 IL-4Rα bound by the blocking Ab. Indeed, engagement of surface IL-4Rα with dupilumab (anti-
157 human IL-4Rα blocking Ab) promotes IL-4Rα internalization via endocytosis, although a
158 dupilumab-bound fraction is also retained on the cell surface (*37*). Nevertheless, the absolute
159 amount of IL-4Rα (both free and blocking Ab-bound) decreases in dupilumab-treated patients,
160 supporting the observed reduction in IL-4Rα expression on OVA$^+$ MBCs in our study (*37*, *38*).
161 Moreover, our transcriptomic analyses indicate a diminished MBC2 phenotype, as both *Fcer2*
162 and *Il4r* expression was significantly decreased in human MBCs that received A4RA treatment.

163 **Long-lived Ag-specific IgG2b/c responses emerge in the absence of IL-4/IL-13 signaling**

164 As we observed that recall responses occurred in the absence of IL-4/IL-13 signaling, alongside
165 dampened MBC2 polarization (including *Ighg1*), we sought to define the Ig product of recall
166 responses. Evaluating isotypes downstream to IgG1 – the dominant memory reservoir in
167 epicutaneously sensitized mice – an increase in *Ighg2b* and *Ighg2c* transcripts was observed in
168 the MBC cluster of A4RA-treated mice (**Fig. 3A**). *Igha* transcript expression was also increased
169 in A4RA-treated mice, though not significantly. Consistent with the notion that IgE^+ MBCs are
170 exceptionally rare or non-existent in mice, mature *Ighe* transcripts were not readily detectable in
171 any experimental group (6 of 7369 cells) (*39–41*). From the paired scVDJ-seq analysis we
172 plotted the assigned *Ighc* gene for each MBC with at least three nucleotide mutations, suggestive
173 of hypermutated, Ag-experienced cells (**Fig. 3B**). The distribution of isotype usage in mutated
174 MBCs was comparable between CT and IC mice, except for *Ighg2b*, which had a substantially
175 greater presence in CT in agreement with the reported CT-induced secretion of TGF-β, a driver
176 of IgG2b CSR (*42*, *43*). By contrast, A4RA induced a pronounced increase in *Ighg2c* above both
177 CT and IC – an isotype that is not associated with type 2 immunity.

178 To assess whether the skewed isotype usage occurred within the Ag-specific B cell repertoire
179 and the longevity of such response, OVA^+ MBCs and the OVA-specific serum Ig profile were
180 interrogated up to 15 weeks after the recall response. OVA^+ $IgG1^+$ MBCs were present in both
181 IC and A4RA-treated mice, though with a significantly decreased frequency with A4RA
182 treatment (**Fig. 3C and 3D**). By comparison, OVA^+ $IgG2c^+$ MBCs emerged with A4RA
183 treatment and were sustained beyond three months. As IgG2c CSR is driven by IFN-γ and our
184 previous work demonstrated an increase in IFN-γ production with A4RA treatment, we sought to
185 establish the role of IFN-γ in the emergence of OVA^+ $IgG2c^+$ MBCs (*18*, *44*, *45*). In mice treated
186 with A4RA, A4RA with concurrent IFN-γ receptor 1 blockade (AIFNGR), or AIFNGR alone,

187 the frequency of OVA^+ B cells was similar, suggesting that IFN-γ signaling does not influence
188 Ag-specific B cell expansion in a recall response (**Fig. 3E**). The emergence of OVA^+ $IgG2c^+$
189 MBCs, however, was halted with concurrent AIFNGR (**Fig. 3F and 3G**).

190 Skewed isotype usage in the absence of IL-4 signaling was also reflected in the analysis of serum
191 OVA-specific Igs (**Fig. 3H**). As per our previous observations, serum OVA-IgE responses were
192 short-lived in IC mice with a completely abrogated response in A4RA-treated mice (*18*, *21*).
193 Consistent with the induction of $IgG2c^+$ MBCs, serum OVA-IgG2c was observed with A4RA
194 treatment though was not long-lived and declined at a similar rate to IgE in IC mice. Disparate to
195 the reduction in OVA^+ $IgG1^+$ MBCs, Ag re-exposure induced a comparable resurgence of serum
196 OVA-IgG1 in both groups, suggesting that A4RA may have limited impact on MBCs fated for
197 PC differentiation. Serum OVA-IgG2b titers were comparable between both groups and OVA-
198 IgA was undetectable.

199 We reasoned that if the skewed isotype response by A4RA was stably maintained then a
200 resurgence of IgG2c should be facilitated by seeded $IgG2c^+$ MBCs. To this end, mice were
201 provided tertiary OVA re-exposures nine weeks post-A4RA/IC and s.c. OVA administration
202 (**Fig. 3I**). At this point there is clearance of both serum OVA-IgG2c and the blocking A4RA Ab
203 (*18*). Indeed, tertiary Ag re-exposure provided a significant regeneration of OVA-IgG2b and
204 OVA-IgG2c though abrogation of OVA-IgE production remained (**Fig. 3J**). Collectively, these
205 data demonstrate that induction of a recall response with IL-4Rα blockade permit the emergence
206 of a non-type 2 Ab response and propose that this reprogrammed B cell response may be
207 maintained even following A4RA clearance.

208 LNs at distinct anatomical sites have been shown to differ in their predisposition to promote
209 inflammatory or tolerogenic responses towards Ags (*46*). In this regard, we also investigated

210 A4RA-induced isotype skewing in the context of oral immunization, which preferentially issues
211 tolerogenic IgA-dominant responses. As previously shown, one intragastric administration of Ag
212 + CT does not issue a humoral response (*47*, *48*), though Ag-specific Igs arise after subsequent
213 oral administration of Ag alone (*47*). We adopted this framework to provide systemic
214 administration of IC or A4RA prior to each oral Ag re-exposure (**fig. S5A**). Expectedly, IC-
215 treated mice exhibited a classical type 2 response marked by OVA^+ $IgG1^+$ MBCs in gut dLNs
216 and serum OVA-IgG1 and -IgE (**fig. S5B and S5C**). Mirroring observations from epicutaneous
217 sensitization, A4RA elicited the emergence of OVA^+ $IgG2c^+$ MBCs and serum OVA-IgG2b and
218 -IgG2c, while preventing OVA-IgE synthesis. Conversely, OVA re-exposures did initiate an IgA
219 response which was abrogated with A4RA, reconciling the requirement of IL-4 signaling for
220 mucosal IgA responses (**fig. S5C**) (*49*). Thus, loss of IL-4/IL-13 signaling during Ag re-exposure
221 preferentially promotes IgG2b/c responses irrespective of tissue site.

222 **Type 1-polarizing adjuvant can redirect isotypic fate of class-switched MBCs arising in**
223 **type 2-polarizing conditions**

224 Having demonstrated that IFN-γ supports the reprogrammed fate of OVA^+ MBCs established in
225 type 2-polarizing conditions, we next assessed whether use of a type 1-polarizing adjuvant could
226 also redirect class-switched MBCs to IgG2b/c.To this end, we utilized an adjuvanted re-exposure
227 system to assess whether the type 1 adjuvant, CpG, can divert the Ag-specific response in type 2
228 immunized mice (**Fig. 4A**). Similar to the effects of A4RA and comparable to that observed in
229 type 1 immunized mice, re-exposure with CpG facilitated an increased frequency of OVA^+
230 $IgG2c^+$ MBCs and a decline in MBC2s, though the heightened frequency of OVA^+ $IgG1^+$ MBCs
231 remained (**Fig. 4B and 4C**). The emergence of $IgG2c^+$ MBCs was also reflected in increased
232 serum titers of OVA-IgG2c, along with OVA-IgG2b (**Fig. 4D**). Remarkably, the type 1-

233 adjuvanted re-exposure did not prevent OVA-IgE production, suggesting that this approach has
234 an attenuated potency in redirecting pathogenic IgE responses relative to A4RA treatment.

235 While A4RA provides direct blockade of IL-4/IL-13 signaling in B cells and T cells, the effect of
236 CpG on CD4 T cells likely operates primarily through an indirect mechanism, involving the
237 modulation of Ag-presenting cells (*50*, *51*). Therefore, we hypothesized that a CpG adjuvanted
238 re-exposure may be more effective in ameliorating the pathogenic IgE fate of MBCs when not
239 having to contend with the existing type 2 bias in Ag-experienced CD4 T cells. To test this, we
240 utilized an adoptive transfer approach in which class-switched OVA-enriched MBCs were sorted
241 from OVA + Alum-immunized CD45.1$^+$ donor mice and were transferred to B cell-deficient
242 (muMT) CD45.2$^+$ naïve mice (**fig. S6A and S6D**). Recipient mice were then immunized with
243 either OVA + CT or OVA + CpG. Of note, OVA + Alum immunization yields an IgG1 and IgE
244 dominant response, where over 85% of the class-switched MBC pool is IgG1$^+$ and less than 4%
245 are IgG2b/c$^+$, with greater than 50% of the IgG1$^+$ also harboring the MBC2 phenotype (*52*) (**fig.
246 S6B and S6C**). Thus, any emergence of OVA-IgG2 responses in recipient mice is not likely to
247 represent an expansion of donor IgG2 clones. Moreover, OVA + CT immunization produces
248 more OVA$^+$ IgG2b/c$^+$ MBCs than Alum; therefore, if any IgG2 clones in the donor pool do
249 contribute to the OVA-IgG2 response in recipients, we would expect to observe this with both
250 CT and CpG immunization (**fig. S6B**).

251 One week following adoptive transfer and immunization, donor (CD45.1$^+$) OVA$^+$ B cells and
252 OVA-specific Igs were detected in recipient mice. As anticipated, immunization of recipient
253 mice with OVA + CT drove the emergence of OVA$^+$ IgG1$^+$ MBCs and serum OVA-IgG1 and -
254 IgE. In contrast, OVA$^+$ IgG2c$^+$ MBCs and serum OVA-IgG2b and -IgG2c became present in
255 recipient mice immunized with OVA + CpG, with a sustained absence of OVA-IgE (**fig. S6E**

256 **and S6F**). Collectively, these data support that Ag re-exposure in the presence of a type 1
257 adjuvant can redirect the fate of class-switched MBCs established under type 2-polarizing
258 conditions.

259 **IgG2c$^+$ B cells arising in a type 1-adjuvanted recall response emerge from GC-derived and**
260 **GC-independent cellular origins**

261 MBCs, including MBC2s, can be generated both extrafollicularly (EF) and as an output of GCs
262 (*14*, *53*). To determine whether EF- or GC-dervied MBCs differentially contribute to the
263 reprogrammed IgE response, we utilized a molecular fate mapping approach with *S1pr2-Igk^{Tag}*
264 mice (*54*). These mice harbor a LoxP-flanked Flag tag and downstream Strep tag at the Igκ light
265 chain gene and Cre^{ERT2} expression under control of the GC-specific *S1pr2* gene (*54*). In this
266 model, B cells and their secreted antibodies express a Flag tag, unless engaged in GCs during
267 tamoxifen (TAM) treatment, at which point the Flag tag is irreversibly replaced with a Strep tag.

268 Following previously established methodology, TAM was administered to *S1pr2-Igk^{Tag}* mice
269 beginning four days after OVA + Alum immunization during GC activity (**Fig. 4E**) (*54*). The
270 product of this primary response yields class-switched cells that are Strep$^+$ if they were GC-
271 derived or Flag$^+$ arising from an EF pathway. Seven days following the final TAM treatment,
272 89.4% of GC B cells were Strep$^+$ (**Fig. 4F**). Of Strep$^+$ GC B cells, 97.4% were IgG1$^+$ and less
273 than 0.25% were IgG2c$^+$, which is in agreement with robust GC activity and IgG1 CSR known to
274 arise in Alum immunization models (*55*). Two months later, following contraction of GC
275 activity, mice were re-exposed to OVA + CpG (without additional TAM treatment) and the
276 OVA$^+$ B cell compartment was analyzed by flow cytometry (**Fig. 4G**). As expected, the
277 overwhelming majority of OVA$^+$ B cells expressing IgD/IgM were Flag$^+$ whereas IgG1$^+$ cells
278 were mostly Strep$^+$, indicative of their GC-derived origin (**Fig. 4G**). OVA$^+$ IgG2c$^+$ B cells,

279 however, exhibited a equal distribution of Flag and Strep expression, suggesting that the IgG2c$^+$
280 B cells emerging in the type 1-adjuvanted recall response can originate from both naïve B cells
281 or EF-derived MBCs (Flag$^+$) and GC-dervied MBCs (Strep$^+$). Given that the product of Alum
282 immunization was overwhelming IgG1-dominant, it is likely that Strep$^+$ IgG2c$^+$ B cells arose
283 from GC-derived IgG1$^+$ MBCs (**fig. S5B**). In this regard, we next tested this possibility by
284 assessing the VDJ repertoire and clonal origins of OVA-specific B cells.

285 **Class switch origins of IgG2b/c$^+$ clones are comprised of multiple isotypes**

286 The observed loss of MBC2 polarization and divergence towards non-IgE humoral response
287 indicate the potential to reprogram pathogenic IgE responses; however, it remains unclear
288 whether skewed isotype usage arises *de novo* (i.e., from naïve or unswitched B cells) or from
289 direct reprogramming of existing class-switched MBCs. To address this, we first looked for the
290 presence of germline sterile transcripts (S-Tx), the expression of which precedes CSR to the
291 productive Ig isotype (*56*, *57*). Thus, the presence of *Ighg2b/c* S-Tx in cells with productive IgM,
292 IgG3, or IgG1 would indicate B cells that are likely primed for IgG2b/c CSR. We used the
293 sciCSR pipeline to annotate S-Tx expression in our scRNA-seq dataset (**Fig. 5A**). S-Tx inclusive
294 of and downstream to *Ighg1* were preferentially expressed in the MBC cluster, congruent with
295 cells in this cluster being Ag-experienced (**Fig. 5B**). *Ighg3* S-Tx were most prevalent in the
296 *Fcrl5*$^+$ cluster which aligns with the observed IgG3 bias in atypical (*Fcrl5*$^+$) MBCs (*58*, *59*).
297 *Ighg2b* S-Tx were also present in naïve-like clusters, perhaps identifying recently activated B
298 cells yet to undergo CSR from IgM.

299 We then asked whether B cells with *Ighg2b/c* S-Tx differed in their gene expression profile
300 relating to cytokine signaling involved in isotype determination during CSR. We found that
301 *Ighg2b/c* S-Tx$^+$ cells had significantly higher expression of genes related to responsiveness to

302 type II IFN and TGF-β, but not type I IFN or IL-4 (**Fig. 5C**). Conversely, cells expressing S-Tx
303 other than *Ighg2b/c* had heightened expression of genes involved in the response to IL-4 relative
304 to S-Tx$^-$ cells.

305 Given that these data indicated a potential for IgG2b/c CSR from naïve and class-switched
306 polyclonal cells, we posited that this would also be true of OVA-specific cells. Accordingly, we
307 next performed scRNA-seq (Smart-Seq2) and bulk VDJ sequencing of OVA-specific B cells
308 sorted from IC- and A4RA-treated mice (**Fig. 5D**). Smart-Seq2 yielded the reconstruction of full
309 length BCRs for 61 and 70 OVA$^+$ B cells from IC- and A4RA-treated mice, respectively. Of the
310 sequenced cells, 70 were class-switched. We employed the same approach described above to
311 investigate the presence of S-Tx in OVA-specific B cells with a productive IgD/M call or IgG1
312 call. With A4RA treatment there was a near complete absence of *Ighe* S-Tx in IgG1$^+$ OVA-
313 specific B cells (2.6% vs. 11.5% of IgG1$^+$ in A4RA and IC, respectively), confirming deterred
314 IgE CSR (**Fig. 5E**). A4RA-treated cells also exhibited a 2-fold increase in OVA$^+$ IgD/M$^+$ B cells
315 expressing *Ighg2c* S-Tx, though the proportion of OVA$^+$ IgG1$^+$ B cells with *Ighg2c* S-Tx was
316 comparable between groups (**Fig. 5E**). The presence *Ighg2b/c* S-Tx was unrelated to the level of
317 SHM in IgD/M$^+$ and IgG1$^+$ cells, suggesting that this is not reflective of increased Ag exposure
318 (**Fig. 5F**). We also further explored the dataset from LSC Il4r-deficiency model and found that
319 the reverse held true – with increased IL-4 bioavailibity, MBCs harbored less *Ighg2b* and *Ighg2c*
320 S-Tx, and increased *Ighe* S-Tx, corroborating that diversion to an IgG2b/c trajectory requires
321 suppressed IL-4 signaling in B cells (**fig.S7A-C**). Notably, A4RA treatment heightened the
322 proportion of both IgD/M$^+$ and IgG1$^+$ cells with *Igha* S-Tx, with increases of 5.4-fold and 4.8-
323 fold, respectively. As there was not a detectable increase in serum OVA-IgA, the increase in
324 *Igha* S-Tx may signal a later propensity for IgA CSR with continued Ag re-exposures.

325 Finally, amongst MBCs with productive *Ighg1*, we compared the expression of genes comprising
326 the IFN-γ receptor heterodimer and their upstream signaling kinases, given our finding that IFN-
327 γ is necessary for the A4RA-induced IgG2c response (**Fig. 3F**). While no difference was
328 observed for *Ifngr2* and its associated signaling kinase *Jak2*, *Ifngr1* and its signaling kinase *Jak1*
329 were significantly upregulated in OVA^+ $Ighg1^+$ MBCs from A4RA-treated mice and were
330 downregulated in MBCs from the LSC Il4r-deficiency model (**Fig. 5G and fig.S7D**). Of
331 relevance, *Ifngr2* is constituvely expressed at low levels, whereas *Ifngr1* expression can be
332 upregulated by pro-inflammatory cytokines, including IFN-γ itself, which coincides with
333 increased IFN-γ production observed in A4RA-treated mice (*60*, *61*).

334 The limited throughput of the Smart-Seq2 approach did not permit the detection of clonally
335 related sequences within either treatment group. In this regard, we utilized bulk VDJ sequencing
336 of OVA-specific B cells sorted from pooled LNs and spleens to assess the clonal ancestry of
337 $Ighg2b/c^+$ cells. Parallel analyses with Ig sequences derived in the 10X dataset were carried out
338 to gain insight as to whether the effects of A4RA are occurring broadly throughout all B cells or
339 are contained within the Ag-specific repertoire. IL-4/IL-13 signaling did not influence CDR3
340 length in unswitched and class-switched B cell repertoires (**fig. S8A and S8B**). Amongst OVA-
341 specific B cells, the extent of SHM was higher in *Ighg1* and *Ighg2b/c* sequences from A4RA-
342 treated mice, which diverges from observations in bulk B cells (**fig. S8C and S8D**). IL-4
343 signaling has been shown to modulate BCL6 expression, leading to the output of GC-derived
344 MBCs (*62*). Therefore, it is possible that blockade of IL-4 signaling permitted sustained GC
345 activity enabling further rounds of SHM in OVA-specific cells. We also observed apparent
346 biases in V gene usage within the class-switched repertoire of OVA-specific B cells (**fig. S8E**);
347 however, this was also present within polyclonal B cells and thus is unlikely related to the OVA-

348 specific recall response (**fig. S8F**). Regarding isotype usage, over 40% of class-switched
349 sequences in the A4RA group were *Ighg2b/c*, compared to only 8% in IC, which coincidences
350 with that observed at the transcriptional, cellular, and protein level (**Fig. 5H**).

351 Broadly probing whether unswitched or class-switched cells were putative precursors to IgG2b/c
352 clones, we first measured the correlation of paired IGHV and IGHJ gene usage between isotypes.
353 Expectedly, paired IGHV-IGHJ gene usage was most highly correlated between *Ighm* and *Ighd*
354 clones in both groups (**fig. S8G**). IGHV-IGHJ gene usage in *Ighg2b/c* clones also correlated
355 most strongly with *Ighm* and *Ighd* clones, and was significantly correlated with *Ighg3* and *Ighg1*
356 clones in A4RA but not IC. Next, we partitioned sequences into clonal lineages through
357 hierarchical clustering, as described previously (*63*, *64*). Amongst trees containing class-
358 switched sequences, 16% of trees in A4RA contained *Ighg2b/c,* versus 2% in IC (**Fig. 5I**).
359 Furthermore, within the *Ighg2b/c*-containing trees in the A4RA group, 57% also included
360 upstream class-switched sequences (*Ighg3* and/or *Ighg1*), confirming a shared clonal lineage
361 between *Ighg2b/c* and other class-switched cells. Accordingly, mutated *Ighg2b/c* sequences were
362 present in B cell lineage trees containing expanded IgM, IgG3, and IgG1 clones (**Fig. 5J**).
363 Collectively, *Ighg2b/c*$^{+}$ cells exhibited clonal relationships with all upstream isotypes,
364 demonstrating that both naïve and class-switched OVA-specific B cells can give rise to IgG2b/c
365 *in vivo*.

366

367 **DISCUSSION**

368 MBCs, compared to naïve counterparts, acquire enhanced functional and metabolic properties
369 increasing fitness for recall responses to the same Ag. The MBCs established upon allergic
370 sensitization gain a unique propensity to switch to IgE upon subsequent allergen exposures,

371 under the influence of IL-4. Whether this specialized B cell memory response is functionally
372 plastic was not yet established. Assessing transcriptional profile, BCR repertoire, Ag-specific
373 cellular memory, and humoral Ab responses, our work identifies the capacity to reprogram the
374 pathogenic IgE-fated response towards a type 1-like, non-pathogenic IgG2c program.

375 Numerous studies in mice and humans have now established that IgG1 is the dominant MBC
376 reservoir for IgE (*5*, *10*, *11*, *21*, *65*). Recent work by us and others has extended upon this
377 concept illustrating that IgE-fated MBCs ("MBC2s") express ε germline transcripts and
378 upregulate surface expression of CD23 and IL-4Rα, seemingly remaining prepared for IL-4
379 responsiveness (*13–15*). In the absence of IL-4/IL-13 signaling in a recall response, we have
380 previously shown that IgE responses are indeed averted, and cytokine production skews toward a
381 Th1 profile (*18*). In the present work investigating how IL-4Rα blockade impacts the B cell
382 repertoire beyond avoidance of IgE production, we found that loss of IL-4/IL-13 signaling *in*
383 *vivo* broadly suppresses gene expression, particularly relating to metabolic processes and BCR
384 signaling. Intriguingly, Ag re-exposure could still elicit Ag-specific GC activity in the absence of
385 IL-4/IL-13, an issue which has remained contentious (*28*, *62*, *66*).

386 As a primary product of a GC response is PC production, we were particularly intrigued by the
387 sustained absence of serum IgE without a compensatory increase in IgG1. Coinciding with our
388 previous observations of an increased IFN-γ to IL-4 ratio, we found that A4RA treatment
389 induced an IFN-γ-dependent Ag-specific IgG2c response, which was otherwise absent with IC.
390 The effector functions of IgG2c are primarily achieved through FcγRI and FcγRIV expressed on
391 myeloid cells (*67*). Engagement with these receptors facilitates effector functions, such as
392 clearance of immune complexes and Ab-dependent cell cytotoxicity, thereby playing an
393 important role in protection against pathogens and a notable absence in type I hypersensitivities.

394 The functional repercussions of an increase in allergen-specific Ab isotypes associated with type
395 1 immunity are yet to be fully understood. However, it stands to reason that both allergen
396 neutralization or Ab-mediated clearance could limit Ag availability for engagement with IgE on
397 mast cells and basophils. In our studies, we found that serum titers of Ag-specific IgG2c were
398 short-lived, however tertiary Ag exposure could re-boost serum IgG2c titers without any
399 observed increase in IgE. Notably, the boosted IgG2c response occurred in the absence of
400 continued IL-4Rα blockade illustrating a sustained reprogramming of the Ag-specific B cell
401 response.

402 The molecular cues which sustain the MBC2 phenotype have not yet been described. In the T
403 cell compartment, a subset of T helper cells, termed "Th2A" is uniquely associated with allergic
404 disease, much like allergen-specific MBC2s (*68*). Th2A cells exhibit heightened Th2-like
405 properties and are terminally differentiated, persisting even with IL-4Rα blockade (*18*, *68*, *69*).
406 Here, we demonstrate that unlike Th2A cells, MBC2s do not harbor a refractory pathogenic
407 phenotype. This requirement of IL-4 to sustain heightened CD23 and IL-4Rα expression was
408 consistent amongst mouse models and humans and reaffirms early observations of IL-4-
409 regulated expression in bulk B cell populations (*36*, *70*). Interestingly, CD23 purportedly
410 augments allergen-specific responses through IgE-facilitated Ag-presentation (*71*, *72*). Thus, it is
411 plausible that depressed CD23 expression observed not only on MBC2s, but throughout the B
412 cell compartment, may curtail reactivation of allergen-specific CD4 T cells.

413 Our analysis of BCR sequences revealed clonal relationships between IgG2b/c and all upstream
414 isotypes, including IgM/D, IgG3, and IgG1. These data, therefore, suggest that both naïve and
415 Ag-experienced B cells can contribute to the A4RA-induced IgG2b/c response. Indeed, using
416 molecular fate mapping we showed that when boosting with a type 1 adjuvant, Ag-specific

417 IgG2c$^+$ B cells can arise from GC-dervied IgG1$^+$ MBCs that were produced during the primary
418 type 2 response. Sequential CSR has been most extensively studied in the IgM to IgE trajectory,
419 where IgG1 is a dominant intermediary. Interestingly, over 50% of the bulk IgG2 repertoire in
420 humans also arises through sequential CSR with an IgG1 intermediary (*73*). This is somewhat
421 surprising given that sequential rounds of V(D)J recombination are likely more metabolically
422 taxing to the host. One explanation for this could be that sequential, rather than direct, CSR
423 provides a means to regulate pro-inflammatory Ab-mediated effector functions. In agreement,
424 both vaccination and allergy yield IgG1 dominant responses, though with chronic Ag exposure
425 through repeated mRNA vaccination or allergen immunotherapy, a shift to the "anti-
426 inflammatory" isotype, IgG4, is observed (*74–78*). Here, we demonstrated that Ag exposure in
427 the absence in IL-4/IL-13 signaling could produce a similar effect – a deviation from the IgG1-
428 IgE axis to an IgG2b/c response. As IgG2b/c is uninvolved in allergic inflammation, this shift to
429 allergen-specific IgG2b/c production could be considered "anti-inflammatory". Nevertheless,
430 clonal relationships between all IgG subclasses and downstream IgE have been reported (*9*);
431 whether the induced non-IgG1-expressing MBCs can later revert to a pathogenic IgE fate in
432 humans is yet to be studied.

433 In summary, we propose the following model through which the IgE-fated B cell response is
434 reshaped in the context of A4RA: 1) Allergic sensitization yields IgG1$^+$ MBCs and type 2-
435 polarized T cells, marked by upregulated IL-4 production. In an unperturbed recall response, IL-
436 4 engages with IL-4R on IgG1$^+$ MBCs enabling IgE CSR. 2) Administration of an IL-4Rα
437 blocking Ab prohibits IL-4 signaling which permits the emergence of a type 1 skewed cytokine
438 response, marked by increased IFN-γ. 3) In this context, naïve and MBCs engage with cognate

439 Ag in a type 1-skewed environment, favoring non-IgE CSR, as well as a loss of the type 2 MBC
440 signature.

441 A limitation of our study is the disparities between mouse and human Ig isotypes, particularly the
442 lack of clear IgG2b/c homologs. In humans, allergen desensitization is most often associated
443 with increases in allergen-specific IgG2 and IgG4 (*75*, *79–81*). Both isotypes only weakly bind
444 Fc receptors relative to other IgG subclasses and thus, may primarily regulate the IgE-mediated
445 pro-inflammatory functions through competition for Ag binding (*82*, *83*). IgG2 is postulated to
446 also regulate IgE effector functions directly through engagement with an inhibitory receptor,
447 CD32b, on mast cells and basophils (*84*). Moreover, the cytokines that direct IgG subclass CSR
448 differ between mice and humans. In mice, IFN-γ alone is necessary for IgG2c CSR, whereas in
449 humans, it is suggested to work in concert with IL-6 and/or IL-2 to direct IgG CSR (*85*, *86*).
450 Although human B cells do express the IFN-γ receptor, its direct signaling appears to mediate
451 spontaneous GC formation and autoantibody production more so than CSR (*87*, *88*). Importantly,
452 however, the MBC2 phenotype is present in both mouse and human allergen-specific $IgG1^+$ B
453 cells (*14*). Accordingly, even though the precise isotype output of a reprogrammed response
454 otherwise fated to become IgE remains elusive, the diminished MBC2 phenotype provides
455 promise of non-IgE CSR. This limitation underscores the importance of conducting parallel
456 studies in humans to determine the reprogrammed fate of allergen-specific MBCs.

457 IL-4Rα blockade (dupilumab) is licensed for the treatment of various atopic diseases, such as
458 moderate-to-serve asthma and chronic rhinosinusitis. Dupilumab significantly reduces serum IgE
459 titers in these contexts, along with a decrease in allergen-specific IgE in trials involving food-
460 allergic patients (*89–94*). Whether this treatment reprograms the pathogenic IgE-fated response
461 has not yet been well addressed. A recent study uncovered that MBC2 frequency declines in

462 atopic dermatitis patients treated with dupilumab, supporting the proposition that IL-4Rα
463 blockade may alter the trajectory of IgE-fated MBCs (*38*). The product of an altered MBC2
464 trajectory in humans and if it is sustained following treatment cessation remains unknown.

465 In summary, our research demonstrates that IL-4/IL-13 signaling is required to sustain the IgE
466 fate of B cell responses in established allergic disease and that loss of IL-4/IL-13 signaling can
467 transform the allergen response to an innocuous type 1 phenotype. This not only bolsters the
468 applicability of anti-IL-4Rα as adjunct therapy to other immunomodulatory interventions, but
469 also broadly illuminates the potential to reprogram deviant B cell responses. Thus, further
470 research is warranted to establish the intrinsic determinants that govern MBC fate, which will be
471 imperative in the development of therapeutic strategies to correct deviant B cell responses in
472 settings like allergy, autoimmunity, and transplantation.

473 **MATERIALS AND METHODS**

474 **Mice**

475 Female C57BL/6 mice (6-8 weeks old) were purchased from Charles River Laboratories
476 (Wilmington, MA). Female B6.129S2-*Ighm*^{tmCgn} and B6.SJL-*Ptprc*^{a} *Pepc*^{b}/Boy mice (6-8 weeks
477 old) were purchased from Jackson Laboratories (Bar Harbor, ME). *Igk*$^{Flag/Strep}$ and *S1pr2-cre*^{ERT2}
478 mice were a generous gift from Dr. Gabriel Victora (The Rockefeller University). All
479 experimentation was in compliance with the McMaster University Research Ethics Board.

480 **Immunizations**

481 *Epicutaneous sensitization:* Epicutaneous sensitization to ovalbumin (Grade V; Sigma-Aldrich,
482 St. Louis, MO) was conducted as previously described (*21*). For recall responses, three low-back
483 subcutaneous injections of 100 μg OVA were given over the course of a week. *Gastric*

484 *sensitization:* Mice received one intragastric gavage of 1 mg OVA with 5 μg cholera toxin (CT)
485 in PBS. Four weeks later, mice received 1 mg OVA in PBS weekly for three weeks via gavage.
486 *Subcutaneous sensitization:* Mice were immunized subcutaneously with 250 μg OVA and 5 μg
487 CT. *Intraperitoneal sensitization:* Mice were immunized intraperitoneally with 250 μg OVA and
488 250 μL Alhydrogel 2% (aluminum hydroxide [alum], InvivoGen, San Diego, CA), 40 μg CpG,
489 or 5 μg CT.

490 Serum for analysis of OVA-specific antibodies was collected through retro-orbital bleeding. For
491 allergen challenges, 5 mg OVA was intraperitoneally injected. Core body temperature and
492 clinical signs were recorded, as previously described, and hematocrit was measured at 40
493 minutes (*95*).

494 **Antibody and Drug Administration**

495 Anti-CD40L (MR-1), anti-IFN-γR1 (GR-20), and anti-trinitrophenol IgG2a isotype control
496 (2A3) were purchased from Bio X Cell (Lebanon, NH). Anti-IL-4Rα (M1) was produced in-
497 house, as previously described (*18*). Original hybridomas were generated by Immunex
498 Corporation (Amgen, Thousand Oaks, CA) and were generously provided by Dr. Fred
499 Finkelman (University of Cincinnati).

500 One mg of anti-IL-4Rα, anti-IFN-γR1, or isotype control was intraperitoneally injected the day
501 prior to s.c. re-exposures. Anti-CD40L (0.35 mg) or isotype control was intraperitoneally
502 injected on days -1, 0, and 2 of s.c. re-exposures.

503 200 μl of 50 mg/ml of tamoixfen (Sigma-Aldrich, Saint Louis, Missouri) was administrated by
504 intragastric gavage on days 4, 8, and 12 post-immunization.

505 **Tetramer Staining and Enrichment**

506 Purified OVA (Sigma-Aldrich, St. Louis, MO) was biotinylated (ThermoFisher Scientific,
507 Waltham, MA) and tetramerized with streptavidin-PE or streptavidin-APC (Agilent, Santa Clara,
508 CA), as previously described (*31*, *32*). For decoy tetramer, β-lactoglobulin (Sigma-Aldrich, St.
509 Louis, MO) was biotinylated. Streptavidin-PE or -APC was conjugated with DyLight 594 or
510 DyLight 755 esters (ThermoFisher Scientific) and was used to tetramerize the biotinylated- β-
511 lactoglobulin.

512 Cell pellets were resuspended and stained with 5 nM decoy tetramer in 20 μL FACS buffer (10%
513 FBS and 1 μM EDTA in PBS) and 2% rat serum for five minutes on ice. Five nM OVA tetramer
514 was added and incubation continued for 30 minutes. Cells were washed to remove unbound
515 tetramer and were incubated with anti-PE or -APC microbeads (Miltenyi Biotec, Germany) for
516 15 minutes on ice. Cells were passed through LS columns affixed to MACS magnetic separator
517 (Miltenyi Biotec). Bound fractions were eluted with FACS buffer.

518 For CD45.1 enrichments, cell pellets were resuspended in 20 μL FACS buffer with 0.25 μg
519 FcBlock (BioLegend) for five minutes on ice, then stained with anti-CD45.1-APC (A20;
520 BioLegend) for 30 minutes. Enrichment with anti-APC microbeads proceeded as described
521 above.

522 **Patient Samples**

523 A cohort of three peanut allergic donors, aged 9-23, were recruited to donate blood from
524 McMaster Children's Hospital and Hamilton Health Sciences (Hamilton, Ontario, Canada).
525 Allergic status was confirmed by peanut-specific IgE (higher than 0.35 kU/L) ImmunoCap at
526 Laboratory Reference Centre Hamilton (McMaster Children's Hospital). Donors were excluded
527 from the study for previous or current allergen immunotherapy, omalizumab, dupilumab or other
528 systemic immunomodulatory treatment, as well as diagnosed autoimmune or immunodeficiency

529 diseases. All donors were recruited with written consent and ethical approval from the Hamilton
530 Integrated Research Ethics Board.

531 Peripheral blood was collected into heparinized tubes (BD). PBMCs were isolated via Ficoll-
532 Paque (GE Healthcare) density centrifugation and were cryopreserved in FBS + 10% DMSO for
533 long-term storage in liquid nitrogen. Before culture, viability of thawed PBMCs was confirmed
534 to be ≥ 70%. PBMCs were cultured for 8 days and stimulated with 2.5 ng/mL crude peanut
535 extract (Stallergenes Greer) with or without 50 ug/mL anti-human IL-4Rα (MAB230; R&D
536 Systems), as previously described (*18*).

537 **Flow Cytometry and Cell Sorting**

538 Single-cell suspensions were plated in U-bottom 96-well plates and incubated with 0.25 µg
539 FcBlock for 10 minutes on ice. Cells were stained extracellularly for 30 minutes on ice with Ab
540 cocktails prepared in FACS buffer. For intracellular staining, cells were fixed and permeabilized
541 with Cytofix/Cytoperm (BD Biosciences), as per manufacturer's instructions. Intracellular Ab
542 cocktails were prepared in 1x perm wash and cells were stained for 30 minutes on ice.

543 The following anti-mouse fluorochrome-conjugated antibodies were used: B220-AF700 (RA3-
544 6B2), CD138-PE/Dazzle 594 (281-2), CD3-BV711 (17A2), CD3-BV510 (17A2), CD45.1-APC
545 (A20), F4/80-BV711 (BM8), F4/80-BV510 (BM8), CD38-PE/Cy7 (90), GL7-PerCP.Cy5.5
546 (GL7), GL7-BV421 (GL7; BD, Franklin Lakes, NJ), IgD-Pacific Blue (11-26c.2a), IgD-BV605
547 (11-26c.2a), IgM-BV786 (II/41; BD), IgM-FITC (II/41), IgG1-BV650 (RMG1-1), IgG2b-PECy7
548 (RMG2b-1), IgG2c-FITC (polyclonal; SouthernBiotech, Birmingham, AL), IL-4Rα-PE
549 (REA235; Miltenyi Biotec), CD23-BV421 (B3B4), Flag-APC (L5), Anti-Streptavidin-Biotin
550 (5A9F9; LSBio, Newark, CA), and Streptavidin-BV421 (405225). The following anti-human
551 antibodies were used: IL-4Rα-PE (G077F6), CD23-BV421 (EBVCS-5), IgD-AF700 (IA6-2),

552 CD27-BV605 (O323), IgM-BV650 (MHM-88), CD38-PECy7 (HB-7), CD19-PerCP.Cy-5.5
553 (SJ25C1), CD3-BV711 (OKT3), CD14-BV711 (M5E2), and CD16-BV711 (3G8). All antibodies
554 were purchased from BioLegend (San Diego, CA), unless otherwise noted. Viability staining
555 was executed with Fixable Viability Dye eFluor780 (eBioscience, San Diego, CA) or Fixable
556 Viability Stain 510 (BD Biosciences).

557 Data were acquired with an LSRFortessa flow cytometer (BD). Bulk cell sorting was performed
558 on a MoFlo XDP cell sorter (Beckman Coulter, Brea, CA). All data were analyzed with FlowJo,
559 version 10 software (Tree Star, Ashland, OR).

560 **Adoptive Transfers**

561 Spleens and mesenteric LNs were collected four weeks following intraperitoneal sensitization of
562 CD45.1^{+} mice with OVA and Alum. Class-switched MBCs (B220^{+} CD3^{-} F4/80^{-} CD38^{+} GL7^{-}
563 IgD^{-} IgM^{-}) from tetramer enriched fractions were isolated by flow sorting. Ten thousand cells
564 were intravenously injected in the tail-vein of naïve recipient (muMT) mice. The day after
565 transfer recipients were intraperitoneally injected with 250 µg OVA with either 40 µg CpG or 5
566 µg CT. One week later, spleens and mesenteric LNs were collected for flow cytometric analysis
567 of donor B cells, and serum was collected for OVA-specific Ig analysis by ELISA.

568 **ELISAs**

569 OVA-specific Igs were measured by sandwich ELISA, described previously, with some
570 modifications (*96*). Briefly, MaxiSorp plates (ThermoFisher Scientifc) were coated with 100 ng
571 anti-IgG2b, -IgG2c, -IgE, or -IgA overnight at 4°C. Plates were blocked in 5% skim milk at
572 37°C for one hour, then diluted (1:2) samples were added and incubated overnight at 4°C.
573 Digoxigenated OVA (15 ng) prepared in-house was added for two hours at room temperature,

574 followed by anti-digoxigenin Fab fragments (Roche, Basel, Switzerland) for one hour. Plates
575 were developed with 3,3',5,5'-tetramethylbenzidinie (Sigma-Aldrich) and stopped with sulfuric
576 acid. Optical densities were acquired with a Multiskan FC photometer (ThermoFisher Scientific).

577 For OVA-IgG1, plates were coated with 400 ng OVA in carbonate-bicarbonate buffer overnight
578 at 4°C. Plates were blocked in 5% skim milk at 37°C for two hours, then diluted (1:20) samples
579 were added and incubated overnight at 4°C. Biotinylated anti-mouse IgG1 (SouthernBiotech;
580 1.25 ng) was added for two hours at room temperature, followed by alkaline-phosphatase
581 streptavidin (ThermoFisher Scientific) for one hour. Plates were developed with 4-nitrophenyl
582 phosphate (Sigma-Aldrich) and stopped with sodium hydroxide. Optical densities were acquired
583 as above.

584 **10x Chromium Sequencing & Analysis**

585 *Sequencing:* Spleens and inguinal LNs were collected one month post-recall response from
586 epicutaneously or subcutaneously sensitized mice and B cells were sorted for sequencing.
587 Single-cell 5' gene expression and V(D)J libraries were prepared with Chromium Single-Cell V3
588 Reagent Kit and Controller (10x Genomics; Pleasanton, CA). Libraries were sequenced with
589 NextSeq2000 (Illumina; San Diego, CA). Data were processed with the Cell Ranger Count and
590 V(D)J pipelines (version 7.0.1).

591 *Gene Expression Analysis:* Sequencing reads were aligned to the mouse transcriptome
592 (GRCm38), followed by filtering, and correction of cell barcodes and Unique Molecular
593 Identifiers (UMIs). Reads associated with retained barcodes were quantified and used to build
594 expression matrices for further analysis with Seurat (version 4.1.3). Cells expressing less than
595 200 genes, genes that were detected in less than 3 cells, and cells expressing over 10%
596 mitochondrial genes were filtered out. Resulting cell counts per condition were CT = 3016, IC =

597 2478, and A4RA = 1875. Data from separate experimental conditions were integrated using
598 reciprocal PCA. Normalization, variable feature selection, and scaling were performed with
599 Seurat default parameters. Principal component analysis (PCA) was performed and the top 15
600 components were used for UMAP dimensionality reduction and clustering at resolution 0.4.
601 Contaminating non-B cells were filtered out and PCA and clustering were repeated on the
602 subsetted Seurat object at resolution 0.3. Differentially expressed genes or gene modules
603 (GO:0006119, R-MMU-983705, GO:0034340, GO:0071559, GO:0034341, GO:0070670) were
604 identified with the Wilcoxon Rank Sum test.

605 *BCR Analysis:* BCR analysis was performed with pipelines in the Immcantation suite (*64*). The
606 "filtered_contig.fasta" and "filtered_contig_annotations.csv" outputs from Cell Ranger V(D)J
607 were used to assign V, D, and J genes with IgBLAST and cells assigned with 0 or >1 heavy
608 chains were removed. Clonal groups were defined with the hierarchialClones function using
609 applying a Hamming distance of 0.1. Germline sequences were reconstructed with
610 createGermlines and IMGT germline references (version 3.1.39). SHM frequency within the
611 IGHV gene was calculated with observedMutations. BAM files from the Cell Ranger output
612 were used to map sterile *Igh* transcripts with the sciCSR pipeline (*97*).

613 **Bulk VDJ Sequencing & Analysis**

614 *Sequencing:* Spleens and inguinal LNs were collected one month post-recall response from
615 epicutaneously sensitized mice and OVA^+ B cells were sorted directly into Buffer RLT (Qiagen;
616 Hilden, DE) prior to shipment on dry ice to iRepertoire. RNA extraction was performed prior to
617 3-chain long read library preparation (Mouse BCR Heavy, Kappa, Lambda). Amplified PCR
618 products were run on MiSeq System with MiSeq Reagent Nano Kit v2 (iRepertoire, Huntsville,
619 AL).

620 *Analysis:* Nucleotide sequences and UMI count were extracted from "joinedSeq" and "copy"
621 columns of the "pep.csv" output from iRweb (iRepertoire) and were aligned with IgBLAST
622 (version 1.18.0) using IMGT reference sequences. Processing of IgBLAST output was
623 performed with the Immcantation suite to assign V, D, and J genes, cluster into clonal groups,
624 assign unmutated germlines, and calculate IGHV SHM hypermutation frequency, as described in
625 the 10x Chromium section. Lineage tree topologies were predicted by maximum parsimony in
626 IgPhyML with constraints for unidirectional isotype switching and trees were subsequently
627 visualized with dowser (*98*, *99*).

628 **Smart-Seq2 Sequencing & Analysis**

629 *Sequencing:* Spleens and inguinal LNs were collected one month post-recall response from
630 epicutaneously sensitized mice. OVA-specific B cells were-single cell sorted into 96 U-bottom
631 well PCR-grade RNase and DNase free plates before being flash frozen at -80C. Full-length
632 cDNA was generated with Smart-Seq Single Cell Kit (Takarabio; Mountain View, CA).
633 Libraries were then prepared for sequencing with NovaSeq 600 Reagent Kits (Illumina;
634 20028400) and sequenced on Illumina NovaSeq 6000 (Ilumina; San Diego, CA).

635 *Analysis:* Sequencing reads were aligned to the mouse transcriptome (GRCm38) with STARsolo
636 (*100*). Count matrix output was normalized and scaled with Seurat (version 4.1.3). Datasets from
637 separate sequencing runs were integrated using reciprocal PCA. BCR sequences were
638 reconstructed with the TRUST4 algorithm to obtain the productive isotype for each cell (*101*,
639 *102*). BAM files from the STARsolo output were then used to map sterile *Igh* transcripts with the
640 sciCSR pipeline (*97*).

641 **Statistical Analysis**

642 Statistical analyses not pertaining to RNA sequencing were performed with Prism 9 (GraphPad
643 Software; San Diego, CA). Comparisons were drawn between groups (CT, IC, A4RA) or across
644 time points using two-sided Student's *t*-test or ANOVA. Data were considered significant with a
645 p value < 0.05.

References

1. R. R. Goel, S. A. Apostolidis, M. M. Painter, D. Mathew, A. Pattekar, O. Kuthuru, S. Gouma, P. Hicks, W. Meng, A. M. Rosenfeld, S. Dysinger, K. A. Lundgreen, L. Kuri-Cervantes, S. Adamski, A. Hicks, S. Korte, D. A. Oldridge, A. E. Baxter, J. R. Giles, M. E. Weirick, C. M. McAllister, J. Dougherty, S. Long, K. D'Andrea, J. T. Hamilton, M. R. Betts, E. T. Luning Prak, P. Bates, S. E. Hensley, A. R. Greenplate, E. J. Wherry, Distinct antibody and memory B cell responses in SARSCoV-2 naïve and recovered individuals following mRNA vaccination. *Sci Immunol* **6**, 1–19 (2021).
2. J. Wrammert, K. Smith, J. Miller, W. A. Langley, K. Kokko, C. Larsen, N. Y. Zheng, I. Mays, L. Garman, C. Helms, J. James, G. M. Air, J. D. Capra, R. Ahmed, P. C. Wilson, Rapid cloning of high-affinity human monoclonal antibodies against influenza virus. *Nature 2008 453:7195* **453**, 667–671 (2008).
3. T. Onodera, Y. Takahashi, Y. Yokoi, M. Ato, Y. Kodama, S. Hachimura, T. Kurosaki, K. Kobayashi, Memory B cells in the lung participate in protective humoral immune responses to pulmonary influenza virus reinfection. *Proc Natl Acad Sci U S A* **109**, 2485–2490 (2012).
4. Z. Yang, B. M. Sullivan, C. D. C. Allen, Fluorescent in vivo detection reveals that IgE(+) B cells are restrained by an intrinsic cell fate predisposition. *Immunity* **36**, 857–72 (2012).
5. R. Jiménez-Saiz, D. K. Chu, T. S. Mandur, T. D. Walker, M. E. Gordon, R. Chaudhary, J. Koenig, S. Saliba, H. J. Galipeau, A. Utley, I. L. King, K. Lee, R. Ettinger, S. Waserman, R. Kolbeck, M. Jordana, Lifelong Memory Responses Perpetuate Humoral Th2 Immunity and Anaphylaxis in Food Allergy. *Journal of Allergy and Clinical Immunology* **140**, 1604–1615 (2017).
6. N. Carballeda-Sangiao, A. I. Rodríguez-Mahillo, M. Careche, A. Navas, I. Moneo, M. González-Muñoz, Changes over Time in IgE Sensitization to Allergens of the Fish Parasite Anisakis spp. *PLoS Negl Trop Dis* **10**, e0004864 (2016).
7. M. S. Kim, M. D. Straesser, B. Keshavarz, L. Workman, E. C. McGowan, T. A. E. Platts-Mills, J. M. Wilson, IgE to galactose-α-1,3-galactose wanes over time in patients who avoid tick bites. *J Allergy Clin Immunol Pract* **8**, 364-367.e2 (2020).
8. D. L. Neuman-Sunshine, J. A. Eckman, C. A. Keet, E. C. Matsui, R. D. Peng, P. J. Lenehan, R. A. Wood, The natural history of persistent peanut allergy. *Annals of Allergy, Asthma & Immunology* **108**, 326-331.e3 (2012).
9. T. J. Looney, J.-Y. Lee, K. M. Roskin, R. A. Hoh, J. King, J. Glanville, Y. Liu, T. D. Pham, C. L. Dekker, M. M. Davis, S. D. Boyd, Human B-cell isotype switching origins of IgE. *J Allergy Clin Immunol* **137**, 579-586.e7 (2016).
10. J.-S. He, S. Subramaniam, V. Narang, K. Srinivasan, S. P. Saunders, D. Carbajo, T. Wen-Shan, N. Hidayah Hamadee, J. Lum, A. Lee, J. Chen, M. Poidinger, F. Zolezzi, J. J. Lafaille, M. A. Curotto de Lafaille, IgG1 memory B cells keep the memory of IgE responses. *Nat Commun* **8**, 641 (2017).
11. I. Hoof, V. Schulten, J. A. Layhadi, T. Stranzl, L. H. Christensen, S. Herrera de la Mata, G. Seumois, P. Vijayanand, C. Lundegaard, K. Niss, A. Lund, J. Ahrenfeldt, J. Holm, E. Steveling, H. Sharif, S. R. Durham, B. Peters, M. H. Shamji, P. S. Andersen, Allergen-specific IgG+ memory B cells are temporally linked to IgE memory responses. *J Allergy Clin Immunol* **146**, 180–191 (2020).
12. A. Vecchione, J. C. Devlin, C. Tasker, V. R. Ramnarayan, P. Haase, E. Conde, D. Srivastava, G. S. Atwal, P. Bruhns, A. J. Murphy, M. A. Sleeman, A. Limnander, W. K. Lim, S. Asrat, J. M. Orengo, IgE plasma cells are transcriptionally and functionally distinct from other isotypes. *Sci Immunol* **9**, 1–15 (2024).
13. C. J. Aranda, E. Gonzalez-Kozlova, S. P. Saunders, W. Fernandes-Braga, M. Ota, S. Narayanan, J. S. He, E. Del Duca, B. Swaroop, S. Gnjatic, G. Shattner, J. Reibman, N. A. Soter, E. Guttman-Yassky, M. A. Curotto de Lafaille, IgG memory B cells expressing IL4R and FCER2 are associated with atopic diseases. *Allergy* **00**, 1–15 (2022).
14. J. F. E Koenig, N. H. Peter Knudsen, A. Phelps, K. Bruton, I. Hoof, G. Lund, D. Della Libera, A. Lund, L. Harder Christensen, D. R. Glass, T. D. Walker, A. Fang, S. Waserman, M. Jordana, P. S. Andersen, "Type 2-polarized memory B cells hold allergen-specific IgE memory" (2024); https://www.science.org.
15. M. Ota, K. B. Hoehn, W. Fernandes-Braga, T. Ota, C. J. Aranda, S. Friedman, M. G. C. Miranda-Waldetario, J. Redes, M. Suprun, G. Grishina, H. A. Sampson, A. Malbari, S. H. Kleinstein, S. H. Sicherer, M. A. Curotto de Lafaille, CD23+IgG1+ memory B cells are poised to switch to pathogenic IgE production in food allergy. *Sci Transl Med* **16**, eadi0673 (2025).

16. F. D. Finkelman, J. F. Urban, M. P. Beckmann, K. A. Schooley, J. M. Holmes, I. M. Katona, Regulation of murine in vivo IgG and IgE responses by a monoclonal anti-IL-4 receptor antibody. *Int Immunol* **3**, 599–607 (1991).
17. F. D. Finkelman, I. M. Katona, J. F. Urban, J. Holmes, J. Ohara, A. S. Tung, J. Sample vG., W. E. Paul, IL-4 is required to generate and sustain in vivo IgE responses. *J Immunol* (1988).
18. K. Bruton, P. Spill, S. Vohra, O. Baribeau, S. Manzoor, S. Gadkar, M. Davidson, T. D. Walker, J. F. E. Koenig, Y. Ellenbogen, A. Florescu, J. Wen, D. K. Chu, S. Waserman, R. Jiménez-Saiz, S. Epelman, C. Robbins, M. Jordana, Interrupting reactivation of immunologic memory diverts the allergic response and prevents anaphylaxis. *J Allergy Clin Immunol* **147**, 1381–1392 (2021).
19. J. K. Nono, H. Ndlovu, N. Abdel Aziz, T. Mpotje, L. Hlaka, F. Brombacher, Interleukin-4 receptor alpha is still required after Th2 polarization for the maintenance and the recall of protective immunity to Nematode infection. *PLoS Negl Trop Dis* **11** (2017).
20. I. M. Katona, J. F. Urban, S. S. Kang, W. E. Paul, F. D. Finkelman, IL-4 requirements for the generation of secondary in vivo IgE responses. *J Immunol* **146**, 4215–21 (1991).
21. R. Jiménez-Saiz, Y. Ellenbogen, J. Koenig, M. E. Gordon, T. D. Walker, D. Rosace, P. Spill, K. Bruton, J. Kong, K. Monteiro, J. Wen, E. I. Tuomanen, R. Kolbeck, D. K. Chu, S. Waserman, M. Jordana, IgG1 $^{+}$ B cell immunity predates IgE responses in epicutaneous sensitization to foods. *Allergy*, doi: 10.1111/all.13481 (2018).
22. K. Haniuda, S. Fukao, D. Kitamura, Metabolic Reprogramming Induces Germinal Center B Cell Differentiation through Bcl6 Locus Remodeling. *Cell Rep* **33** (2020).
23. L. R. Waters, F. M. Ahsan, D. M. Wolf, O. Shirihai, M. A. Teitell, Initial B Cell Activation Induces Metabolic Reprogramming and Mitochondrial Remodeling. *iScience* **5**, 99 (2018).
24. R. Noelle, P. H. Krammer, J. Ohara, J. W. Uhr, E. S. Vitetta, Increased expression of Ia antigens on resting B cells: an additional role for B-cell growth factor. *Proceedings of the National Academy of Sciences* **81**, 6149–6153 (1984).
25. S. R. Dillon, C. Sprecher, A. Hammond, J. Bilsborough, M. Rosenfeld-Franklin, S. R. Presnell, H. S. Haugen, M. Maurer, B. Harder, J. Johnston, S. Bort, S. Mudri, J. L. Kuijper, T. Bukowski, P. Shea, D. L. Dong, M. Dasovich, F. J. Grant, L. Lockwood, S. D. Levin, C. LeCiel, K. Waggie, H. Day, S. Topouzis, J. Kramer, R. Kuestner, Z. Chen, D. Foster, J. Parrish-Novak, J. A. Gross, Interleukin 31, a cytokine produced by activated T cells, induces dermatitis in mice. *Nature Immunology 2004 5:7* **5**, 752–760 (2004).
26. D. Chen, Y. Wang, G. K. Manakkat Vijay, S. Fu, C. W. Nash, D. Xu, D. He, N. Salomonis, H. Singh, H. Xu, Coupled analysis of transcriptome and BCR mutations reveals role of OXPHOS in affinity maturation. *Nature Immunology 2021 22:7* **22**, 904–913 (2021).
27. S. C. Choi, L. Morel, Immune metabolism regulation of the germinal center response. *Experimental & Molecular Medicine 2020 52:3* **52**, 348–355 (2020).
28. A. Turqueti-Neves, M. Otte, O. P. da Costa, U. E. Höpken, M. Lipp, T. Buch, D. Voehringer, B-cell-intrinsic STAT6 signaling controls germinal center formation. *Eur J Immunol* **44**, 2130–2138 (2014).
29. G. v Zuccarino-Catania, S. Sadanand, F. J. Weisel, M. M. Tomayko, H. Meng, S. H. Kleinstein, K. L. Good-Jacobson, M. J. Shlomchik, CD80 and PD-L2 define functionally distinct memory B cell subsets that are independent of antibody isotype. *Nat Immunol* **15**, 631–637 (2014).
30. A. F. Cunningham, K. Serre, K. M. Toellner, M. Khan, J. Alexander, F. Brombacher, I. C. M. MacLennan, Pinpointing IL-4-independent acquisition and IL-4-influenced maintenance of Th2 activity of CD4 T cells. *Eur J Immunol* **34**, 686–694 (2004).
31. J. J. Taylor, R. J. Martinez, P. J. Titcombe, L. O. Barsness, S. R. Thomas, N. Zhang, S. D. Katzman, M. K. Jenkins, D. L. Mueller, Deletion and anergy of polyclonal B cells specific for ubiquitous membrane-bound self-antigen. *J Exp Med* **209**, 2065–77 (2012).
32. A. Phelps, D. Pazos-Castro, F. Urselli, E. Grydziuszko, O. Mann-Delany, A. Fang, T. D. Walker, R. T. Guruge, J. Tome-Amat, A. Diaz-Perales, S. Waserman, J. Boonyaratanakornkit, M. Jordana, J. J. Taylor, J. F. E. Koenig, Production and use of antigen tetramers to study antigen-specific B cells. *Nat Protoc* **19**, 727–751 (2024).
33. J. J. Taylor, K. A. Pape, M. K. Jenkins, A germinal center-independent pathway generates unswitched memory B cells early in the primary response. *J Exp Med* **209**, 597–606 (2012).
34. L. Duan, D. Liu, H. Chen, M. A. Mintz, M. Y. Chou, D. I. Kotov, Y. Xu, J. An, B. J. Laidlaw, J. G. Cyster, Follicular dendritic cells restrict interleukin-4 availability in germinal centers and foster memory B cell generation. *Immunity* **54**, 2256-2272.e6 (2021).

752 35. J. D. Mountz, M. Gao, D. M. Ponder, S. Liu, C. W. Sun, F. Alduraibi, K. Sullivan, B. Pat, L. J. Dell'Italia,
753 H. C. Hsu, IL-4 receptor blockade is a global repressor of naïve B cell development and responses in a
754 dupilumab-treated patient. *Clin Immunol* **244** (2022).
755 36. M. Sarfati, S. Fournier, M. Christoffersen, G. Biron, Expression of CD23 antigen and its regulation by IL-4
756 in chronic lymphocytic leukemia. *Leuk Res* **14**, 47–55 (1990).
757 37. L. E. M. Heeb, O. Boyman, Comprehensive analysis of human IL-4 receptor subunits shows
758 compartmentalization in steady state and dupilumab treatment. *Allergy* **78**, 1073–1087 (2023).
759 38. M. E. Starrenburg, M. Bel Imam, J. F. Lopez, L. Buergi, N. T. Nguyen, A. E. M. Nouwen, N. J. T. Arends,
760 P. J. Caspers, M. Akdis, S. G. M. A. Pasmans, W. van de Veen, Dupilumab treatment decreases MBC2s,
761 correlating with reduced IgE levels in pediatric atopic dermatitis. *Journal of Allergy and Clinical*
762 *Immunology* **154**, 1333-1338.e4 (2024).
763 39. J.-S. He, M. Meyer-Hermann, D. Xiangying, L. Y. Zuan, L. A. Jones, L. Ramakrishna, V. C. de Vries, J.
764 Dolpady, H. Aina, S. Joseph, S. Narayanan, S. Subramaniam, M. Puthia, G. Wong, H. Xiong, M. Poidinger,
765 J. F. Urban, J. J. Lafaille, M. A. Curotto de Lafaille, The distinctive germinal center phase of IgE+ B
766 lymphocytes limits their contribution to the classical memory response. *Journal of Experimental Medicine*
767 **210**, 2755–2771 (2013).
768 40. Z. Yang, M. J. Robinson, C. D. C. Allen, Regulatory constraints in the generation and differentiation of IgE-
769 expressing B cells. *Curr Opin Immunol* **28**, 64–70 (2014).
770 41. R. Jiménez-Saiz, D. K. Chu, T. S. Mandur, T. D. Walker, M. E. Gordon, R. Chaudhary, J. Koenig, S. Saliba,
771 H. J. Galipeau, A. Utley, I. L. King, K. Lee, R. Ettinger, S. Waserman, R. Kolbeck, M. Jordana, Lifelong
772 Memory Responses Perpetuate Humoral Th2 Immunity and Anaphylaxis in Food Allergy. *Journal of*
773 *Allergy and Clinical Immunology* **140**, 1604–1615 (2017).
774 42. A. K. Gloudemans, M. Plantinga, M. Guilliams, M. A. Willart, A. Ozir-Fazalalikhan, A. van der Ham, L.
775 Boon, N. L. Harris, H. Hammad, H. C. Hoogsteden, M. Yazdanbakhsh, R. W. Hendriks, B. N. Lambrecht,
776 H. H. Smits, The Mucosal Adjuvant Cholera Toxin B Instructs Non-Mucosal Dendritic Cells to Promote
777 IgA Production Via Retinoic Acid and TGF-β. *PLoS One* **8**, e59822 (2013).
778 43. T. M. McIntyre, D. R. Klinma, P. Rohman, M. Lugo, J. R. Dasch, J. J. Mond, C. M. Snapper, Transforming
779 growth factor beta 1 selectivity stimulates immunoglobulin G2b secretion by lipopolysaccharide-activated
780 murine B cells. *Journal of Experimental Medicine* **177**, 1031–1037 (1993).
781 44. C. M. Snapper, W. E. Paul, Interferon-γ and B Cell Stimulatory Factor-1 Reciprocally Regulate Ig Isotype
782 Production. *Science (1979)* **236**, 944–947 (1987).
783 45. A. Bossie, E. S. Vitetta, IFN-gamma enhances secretion of IgG2a from IgG2a-committed LPS-stimulated
784 murine B cells: implications for the role of IFN-gamma in class switching. *Cell Immunol* **135**, 95–104
785 (1991).
786 46. D. Esterházy, M. C. C. Canesso, L. Mesin, P. A. Muller, T. B. R. de Castro, A. Lockhart, M. ElJalby, A. M.
787 C. Faria, D. Mucida, Compartmentalized gut lymph node drainage dictates adaptive immune responses.
788 *Nature 2019 569:7754* **569**, 126–130 (2019).
789 47. B. Zhang, E. Liu, J. A. Gertie, J. Joseph, L. Xu, E. Y. Pinker, D. A. Waizman, J. Catanzaro, K. H. Hamza,
790 K. Lahl, U. Gowthaman, S. C. Eisenbarth, Divergent T follicular helper cell requirement for IgA and IgE
791 production to peanut during allergic sensitization. *Sci Immunol* **5** (2020).
792 48. Q. Chen, M. Xie, H. Liu, A. L. Dent, Development of allergen-specific IgE in a food-allergy model requires
793 precisely timed B cell stimulation and is inhibited by Fgl2. *Cell Rep* **39**, 110990 (2022).
794 49. M. Vajdy, M. H. Kosco-Vilbois, M. Kopf, G. Köhler, N. Lycke, Impaired mucosal immune responses in
795 interleukin 4-targeted mice. *J Exp Med* **181**, 41–53 (1995).
796 50. K. Kranzer, M. Bauer, G. B. Lipford, K. Heeg, H. Wagner, R. Lang, CpG-oligodeoxynucleotides enhance T-
797 cell receptor-triggered interferon-γ production and up-regulation of CD69 via induction of antigen-
798 presenting cell-derived interferon type T and interleukin-12. *Immunology* **99**, 170–178 (2000).
799 51. S. Sun, X. Zhang, D. F. Tough, J. Sprent. Type I Interferon-mediated Stimulation of T Cells by CpG DNA. *J*
800 *Exp* Med **188** (12), 2335-2342 (1998).
801 52. Z. Yang, C.-A. M. Wu, S. Targ, C. D. C. Allen, IL-21 is a broad negative regulator of IgE class switch
802 recombination in mouse and human B cells. *Journal of Experimental Medicine* **217** (2020).
803 53. R. A. Elsner, M. J. Shlomchik, Germinal Center and Extrafollicular B Cell Responses in Vaccination,
804 Immunity, and Autoimmunity. *Immunity* **53** (6), 1136-1150 (2020).
805 54. A. Schiepers, M. F. L. van 't Wout, A. J. Greaney, T. Zang, H. Muramatsu, P. J. C. Lin, Y. K. Tam, L.
806 Mesin, T. N. Starr, P. D. Bieniasz, N. Pardi, J. D. Bloom, G. D. Victora, Molecular fate-mapping of serum
807 antibody responses to repeat immunization. *Nature* **615**, 482–489 (2023).

808 55. Z. Yang, C. A. M. Wu, S. Targ, C. D. C. Allen, IL-21 is a broad negative regulator of IgE class switch
809 recombination in mouse and human B cells. *Journal of Experimental Medicine* **217** (2020).
810 56. J. Stavnezer, J. E. J. Guikema, C. E. Schrader. Mechanism and regulation of class switch recombination.
811 *Ann Rev Immunol* **26**, 261-92 (2008).
812 57. T. Honjo, M. Reth, A. Radbruch, F. Alt, M. Neuberger, *Molecular Biology of B Cells* (Academic Press,
813 2004; https://books.google.ca/books?id=fF8d3eZ6SZ8C).
814 58. H. J. Sutton, R. Aye, A. H. Idris, R. Vistein, E. Nduati, O. Kai, J. Mwacharo, X. Li, X. Gao, T. D. Andrews,
815 M. Koutsakos, T. H. O. Nguyen, M. Nekrasov, P. Milburn, A. Eltahla, A. A. Berry, N. KC, S. Chakravarty,
816 B. K. L. Sim, A. K. Wheatley, S. J. Kent, S. L. Hoffman, K. E. Lyke, P. Bejon, F. Luciani, K. Kedzierska,
817 R. A. Seder, F. M. Ndungu, I. A. Cockburn, Atypical B cells are part of an alternative lineage of B cells that
818 participates in responses to vaccination and infection in humans. *Cell Rep* **34** (2021).
819 59. N. Obeng-Adjei, S. Portugal, P. Holla, S. Li, H. Sohn, A. Ambegaonkar, J. Skinner, G. Bowyer, O. K.
820 Doumbo, B. Traore, S. K. Pierce, P. D. Crompton, Malaria-induced interferon-γ drives the expansion of
821 Tbethi atypical memory B cells. *PLoS Pathog* **13**, e1006576- (2017).
822 60. C. Chen, L. Guo, M. Shi, M. Hu, M. Hu, M. Yu, T. Wang, L. Song, B. Shen, L. Qian, N. Guo, Modulation
823 of IFN-γ Receptor 1 Expression by AP-2α Influences IFN-γ Sensitivity of Cancer Cells. *Am J Pathol* **180**,
824 661–671 (2012).
825 61. K. Bruton, P. Spill, S. Vohra, O. Baribeau, S. Manzoor, S. Gadkar, M. Davidson, T. D. Walker, J. F. E.
826 Koenig, Y. Ellenbogen, A. Florescu, J. Wen, D. K. Chu, S. Waserman, R. Jiménez-Saiz, S. Epelman, C.
827 Robbins, M. Jordana, Interrupting reactivation of immunologic memory diverts the allergic response and
828 prevents anaphylaxis. *J Allergy Clin Immunol* **147**, 1381–1392 (2021).
829 62. L. Shehata, C. D. Thouvenel, B. D. Hondowicz, L. A. Pew, G. H. Pritchard, D. J. Rawlings, J. Choi, M.
830 Pepper, Interleukin-4 downregulates transcription factor BCL6 to promote memory B cell selection in
831 germinal centers. *Immunity* **57**, 843-858.e5 (2024).
832 63. Z. Chen, A. M. Collins, Y. Wang, B. A. Gata, Clustering-based identification of clonally-related
833 immunoglobulin gene sequence sets. *Immunome Res* **6**, 1–7 (2010).
834 64. N. T. Gupta, J. A. Vander Heiden, M. Uduman, D. Gadala-Maria, G. Yaari, S. H. Kleinstein, Change-O: a
835 toolkit for analyzing large-scale B cell immunoglobulin repertoire sequencing data. *Bioinformatics* **31**,
836 3356–3358 (2015).
837 65. R. Jiménez-Saiz, Y. Ellenbogen, K. Bruton, P. Spill, D. D. Sommer, H. Lima, S. Waserman, S. U. Patil, W.
838 G. Shreffler, M. Jordana, Human BCR analysis of single-sorted, putative IgE+ memory B cells in food
839 allergy. *J Allergy Clin Immunol* **144**, 336-339.e6 (2019).
840 66. D. G. Gonzalez, C. M. Cote, J. R. Patel, C. B. Smith, Y. Zhang, K. M. Nickerson, T. Zhang, S. M. Kerfoot,
841 A. M. Haberman, Nonredundant Roles of IL-21 and IL-4 in the Phased Initiation of Germinal Center B
842 Cells and Subsequent Self-Renewal Transitions. *J Immunol* **201**, 3569–3579 (2018).
843 67. A. Zhang, H. D. Stacey, M. R. D'Agostino, Y. Tugg, A. Marzok, M. S. Miller, Beyond neutralization: Fc-
844 dependent antibody effector functions in SARS-CoV-2 infection. *Nat Rev Immunol* **23**(6), 381-396 (2023).
845 68. E. Wambre, V. Bajzik, J. H. DeLong, K. O'Brien, Q.-A. Nguyen, C. Speake, V. H. Gersuk, H. A. DeBerg,
846 E. Whalen, C. Ni, M. Farrington, D. Jeong, D. Robinson, P. S. Linsley, B. P. Vickery, W. W. Kwok, A
847 phenotypically and functionally distinct human TH2 cell subpopulation is associated with allergic disorders.
848 *Sci Transl Med* **9**, eaam9171 (2017).
849 69. C. Bangert, K. Rindler, T. Krausgruber, N. Alkon, F. M. Thaler, H. Kurz, T. Ayub, D. Demirtas, N.
850 Fortelny, V. Vorstandlechner, W. M. Bauer, T. Quint, M. Mildner, C. Jonak, A. Elbe-Bürger, J. Griss, C.
851 Bock, P. M. Brunner, Persistence of mature dendritic cells, T_H2A, and Tc2 cells characterize clinically
852 resolved atopic dermatitis under IL-4Rα blockade. *Sci Immunol* **6** (2021).
853 70. H. Renz, J. Domenico, E. W. Gelfand, IL-4-dependent up-regulation of IL-4 receptor expression in murine T
854 and B cells. *Journal of Immunology* **146**, 3049–3055 (1991).
855 71. J. Holm, N. Willumsen, P. A. Würtzen, L. H. Christensen, K. Lund, Facilitated antigen presentation and its
856 inhibition by blocking IgG antibodies depends on IgE repertoire complexity. *J Allergy Clin Immunol* **127**,
857 1029–37 (2011).
858 72. C. Liu, K. Richard, M. Wiggins, X. Zhu, D. H. Conrad, W. Song, CD23 can negatively regulate B-cell
859 receptor signaling. *Sci Rep* **6**, 25629 (2016).
860 73. F. Horns, C. Vollmers, D. Croote, S. F. Mackey, G. E. Swan, C. L. Dekker, M. M. Davis, S. R. Quake,
861 Lineage tracing of human B cells reveals the in vivo landscape of human antibody class switching. *Elife* **5**
862 (2016).

74. P. Irrgang, J. Gerling, K. Kocher, D. Lapuente, P. Steininger, K. Habenicht, M. Wytopil, S. Beileke, S. Schäfer, J. Zhong, G. Ssebyatika, T. Krey, V. Falcone, C. Schülein, A. S. Peter, K. Nganou-Makamdop, H. Hengel, J. Held, C. Bogdan, K. Überla, K. Schober, T. H. Winkler, M. Tenbusch, Class switch toward noninflammatory, spike-specific IgG4 antibodies after repeated SARS-CoV-2 mRNA vaccination. *Sci Immunol* **8** (2023).
75. J. J. Heeringa, C. I. McKenzie, N. Varese, M. Hew, A. T. C. M. Bakx, P. M. Aui, J. M. Rolland, R. E. O'Hehir, M. C. van Zelm, Induction of IgG2 and IgG4 B-cell memory following sublingual immunotherapy for ryegrass pollen allergy. *Allergy* **75**, 1121 (2020).
76. B. P. Vickery, J. Lin, M. Kulis, Z. Fu, P. H. Steele, S. M. Jones, A. M. Scurlock, G. Gimenez, L. Bardina, H. A. Sampson, A. W. Burks, Peanut oral immunotherapy modifies IgE and IgG4 responses to major peanut allergens. *J Allergy Clin Immunol* **131**, 128-34.e1–3 (2013).
77. P. Varshney, S. M. Jones, A. M. Scurlock, T. T. Perry, A. Kemper, P. Steele, A. Hiegel, J. Kamilaris, S. Carlisle, X. Yue, M. Kulis, L. Pons, B. Vickery, A. W. Burks, A randomized controlled study of peanut oral immunotherapy: clinical desensitization and modulation of the allergic response. *J Allergy Clin Immunol* **127**, 654–60 (2011).
78. T. Rispens, M. G. Huijbers, The unique properties of IgG4 and its roles in health and disease. *Nature Reviews Immunology 2023 23:11* **23**, 763–778 (2023).
79. M. Sugimoto, N. Kamemura, M. Nagao, M. Irahara, S. Kagami, T. Fujisawa, H. Kido, Differential response in allergen-specific IgE, IgGs, and IgA levels for predicting outcome of oral immunotherapy. *Pediatr Allergy Immunol* **27**, 276–282 (2016).
80. O. T. Burton, S. L. Logsdon, J. S. Zhou, J. Medina-Tamayo, A. Abdel-Gadir, M. Noval Rivas, K. J. Koleoglou, T. A. Chatila, L. C. Schneider, R. Rachid, D. T. Umetsu, H. C. Oettgen, Oral immunotherapy induces IgG antibodies that act via FcγRIIb to suppress IgE-mediated hypersensitivity. *J Allergy Clin Immunol* **134**, 1310 (2014).
81. P. Satitsuksanoa, W. van de Veen, G. Tan, J. F. Lopez, O. Wirz, K. Jansen, M. Sokolowska, D. Mirer, A. Globinska, T. Boonpiyathad, S. R. Schneider, E. Barletta, H. Spits, I. Chang, H. Babayev, İ. Tahralı, G. Deniz, E. Ö. Yücel, A. Kıykım, S. D. Boyd, C. A. Akdis, K. Nadeau, M. Akdis, Allergen-specific B cell responses in oral immunotherapy-induced desensitization, remission, and natural outgrowth in cow's milk allergy. *Allergy: European Journal of Allergy and Clinical Immunology*, doi: 10.1111/all.16220 (2024).
82. B. G. De Jong, H. Ijspeert, L. Marques, M. Van Der Burg, J. J. M. Van Dongen, B. G. Loos, M. C. Van Zelm, Human IgG2- and IgG4-expressing memory B cells display enhanced molecular and phenotypic signs of maturity and accumulate with age. *Immunol Cell Biol* **95**, 744 (2017).
83. A. M. Collins, K. J. L. Jackson, A Temporal Model of Human IgE and IgG Antibody Function. *Front Immunol* **4** (2013).
84. D. MacGlashan, R. G. Hamilton, Parameters Determining the Efficacy of CD32 to Inhibit Activation of FcεRI in Human Basophils. *J Allergy Clin Immunol* **137**, 1256 (2016).
85. A. Kitani, W. Strober, Regulation of C gamma subclass germ-line transcripts in human peripheral blood B cells. *Journal of immunology* **151 7**, 3478–88 (1993).
86. Y. Kawano, T. Noma, Role of interleukin-2 and interferon-γ in inducing production of IgG subclasses in lymphocytes of human newborns. *Immunology* **88**, 40–48 (1996).
87. P. P. Domeier, S. B. Chodisetti, C. Soni, S. L. Schell, M. J. Elias, E. B. Wong, T. K. Cooper, D. Kitamura, Z. S. M. Rahman, IFN-γ receptor and STAT1 signaling in B cells are central to spontaneous germinal center formation and autoimmunity. *Journal of Experimental Medicine* **213**, 715–732 (2016).
88. P. Kochayoo, P. Thawornpan, K. Wangriatisak, S. Changrob, C. Leepiyasakulchai, L. Khowawisetsut, J. H. Adams, P. Chootong, Interferon-γ signal drives differentiation of T-bethi atypical memory B cells into plasma cells following Plasmodium vivax infection. *Sci Rep* **12** (2022).
89. R. S. Chinthrajah, S. B. Sindher, K. C. Nadeau, J. G. Leflein, J. M. Spergel, D. H. Petroni, S. M. Jones, T. B. Casale, J. Wang, W. W. Carr, W. G. Shreffler, R. A. Wood, E. Wambre, J. Liu, B. Akinlade, A. Atanasio, J. M. Orengo, J. D. Hamilton, M. A. Kamal, A. T. Hooper, K. Patel, E. Laws, L. P. Mannent, D. C. Adelman, A. Ratnayake, A. R. Radin, Dupilumab as an Adjunct to Oral Immunotherapy in Pediatric Patients With Peanut Allergy. *Allergy: European Journal of Allergy and Clinical Immunology*, doi: 10.1111/all.16420 (2024).
90. L. P. van der Rijst, M. S. Hilbrands, N. P. A. Zuithoff, M. S. de Bruin-Weller, A. C. Knulst, T. M. Le, M. de Graaf, Dupilumab induces a significant decrease of food specific immunoglobulin E levels in pediatric atopic dermatitis patients. John Wiley and Sons Inc [Preprint] (2024). https://doi.org/10.1002/clt2.12381.

91. K. Jonstam, B. N. Swanson, L. P. Mannent, L. O. Cardell, N. Tian, Y. Wang, D. Zhang, C. Fan, G. Holtappels, J. D. Hamilton, A. Grabher, N. M. H. Graham, G. Pirozzi, C. Bachert, Dupilumab reduces local type 2 pro-inflammatory biomarkers in chronic rhinosinusitis with nasal polyposis. *Allergy: European Journal of Allergy and Clinical Immunology* **74**, 743–752 (2019).
92. J. D. Hamilton, S. Harel, B. N. Swanson, W. Brian, Z. Chen, M. S. Rice, N. Amin, M. Ardeleanu, A. Radin, B. Shumel, M. Ruddy, N. Patel, G. Pirozzi, L. Mannent, N. M. H. Graham, Dupilumab suppresses type 2 inflammatory biomarkers across multiple atopic, allergic diseases. *Clinical and Experimental Allergy* **51**, 915–931 (2021).
93. L. A. Beck, A. Muraro, M. Boguniewicz, Z. Chen, J. Zahn, A. Rodríguez Marco, Dupilumab reduces inflammatory biomarkers in pediatric patients with moderate-to-severe atopic dermatitis. *Journal of Allergy and Clinical Immunology* **155**, 135–143 (2025).
94. M. Castro, J. Corren, I. D. Pavord, J. Maspero, S. Wenzel, K. F. Rabe, W. W. Busse, L. Ford, L. Sher, J. M. FitzGerald, C. Katelaris, Y. Tohda, B. Zhang, H. Staudinger, G. Pirozzi, N. Amin, M. Ruddy, B. Akinlade, A. Khan, J. Chao, R. Martincova, N. M. H. Graham, J. D. Hamilton, B. N. Swanson, N. Stahl, G. D. Yancopoulos, A. Teper, Dupilumab Efficacy and Safety in Moderate-to-Severe Uncontrolled Asthma. *New England Journal of Medicine* **378**, 2486–2496 (2018).
95. K. Arias, D. K. Chu, K. Flader, F. Botelho, T. D. Walker, N. Arias, A. A. Humbles, A. J. Coyle, H. C. Oettgen, H.-D. Chang, N. van Rooijen, S. Waserman, M. Jordana, Distinct immune effector pathways contribute to the full expression of peanut-induced anaphylactic reactions in mice. *J Allergy Clin Immunol* **127**, 1552–61.e1 (2011).
96. J. Sun, K. Arias, D. Alvarez, R. Fattouh, T. Walker, S. Goncharova, B. Kim, S. Waserman, J. Reed, A. J. Coyle, M. Jordana, Impact of CD40 Ligand, B Cells, and Mast Cells in Peanut-Induced Anaphylactic Responses. *The Journal of Immunology* **179** (2007).
97. J. C. F. Ng, G. Montamat Garcia, A. T. Stewart, P. Blair, C. Mauri, D. K. Dunn-Walters, F. Fraternali, sciCSR infers B cell state transition and predicts class-switch recombination dynamics using single-cell transcriptomic data. *Nat Methods* **21**, 823–834 (2024).
98. K. B. Hoehn, J. A. Vander Heiden, J. Q. Zhou, G. Lunter, O. G. Pybus, S. H. Kleinstein, Repertoire-wide phylogenetic models of B cell molecular evolution reveal evolutionary signatures of aging and vaccination. *Proc Natl Acad Sci U S A* **116**, 22664–22672 (2019).
99. K. B. Hoehn, O. G. Pybus, S. H. Kleinstein, Phylogenetic analysis of migration, differentiation, and class switching in B cells. *PLoS Comput Biol* **18** (2022).
100. B. Kaminow, D. Yunusov, A. Dobin, STARsolo: accurate, fast and versatile mapping/quantification of single-cell and single-nucleus RNA-seq data. *bioRxiv*, 2021.05.05.442755 (2021).
101. L. Song, D. Cohen, Z. Ouyang, Y. Cao, X. Hu, X. S. Liu, TRUST4: immune repertoire reconstruction from bulk and single-cell RNA-seq data. *Nature Methods 2021 18:6* **18**, 627–630 (2021).
102. A. Yermanos, A. Agrafiotis, R. Kuhn, D. Robbiani, J. Yates, C. Papadopoulou, J. Han, I. Sandu, C. Weber, F. Bieberich, R. Vazquez-Lombardi, A. Dounas, D. Neumeier, A. Oxenius, S. T. Reddy, Platypus: an open-access software for integrating lymphocyte single-cell immune repertoires with transcriptomes. *NAR Genom Bioinform* **3** (2021).

Acknowledgments: We kindly thank S. Eisenbarth for thoughtful review of the manuscript. We also thank M. Subapanditha for assistance with cell sorting and C. Mader, the McMaster Genomics Facility, and G. Kongsgaard Koed, and J. Skovsgaard for sequencing support. We thank J. Ng for guidance with sciCSR pipeline. Experimental schematics were created with BioRender (www.biorender.com). KB was supported by a CIHR CGS-Doctoral award and CIHR Postdoctoral Fellowship. AP was supported by the Schroder

Allergy & Immunology Research Institute Scholarship and an Ontario Graduate Scholarship.

Funding:

Schroeder Foundation (SW, MJ)

Food Allergy Canada (SW, MJ)

ALK Abelló (SW, MJ)

Canadian Allergy, Asthma, and Immunology Foundation (MJ)

Michael Zych Family (SW, MJ)

Author contributions:

Conceptualization: KB, AP, MJ

Investigation: KB, AP, AA, AF, TDW, JW, SSK-B, DDL, OM-D, SG, EG, JFEK, AG

Visualization: KB, AP

Funding acquisition: SW, PSA, MJ

Supervision: MJ

Writing – original draft: KB, AP

Writing – review & editing: KB, AP, MJ

Competing interests: JFEK, SW, and MJ receive funding from ALK Abelló A/S. All other authors declare that they have no competing interests.

Data and materials availability: This manuscript produced no new code. Single-cell and bulk sequencing data will be deposited to the GEO database prior to publication. All other data are available within the main text or the supplementary materials.

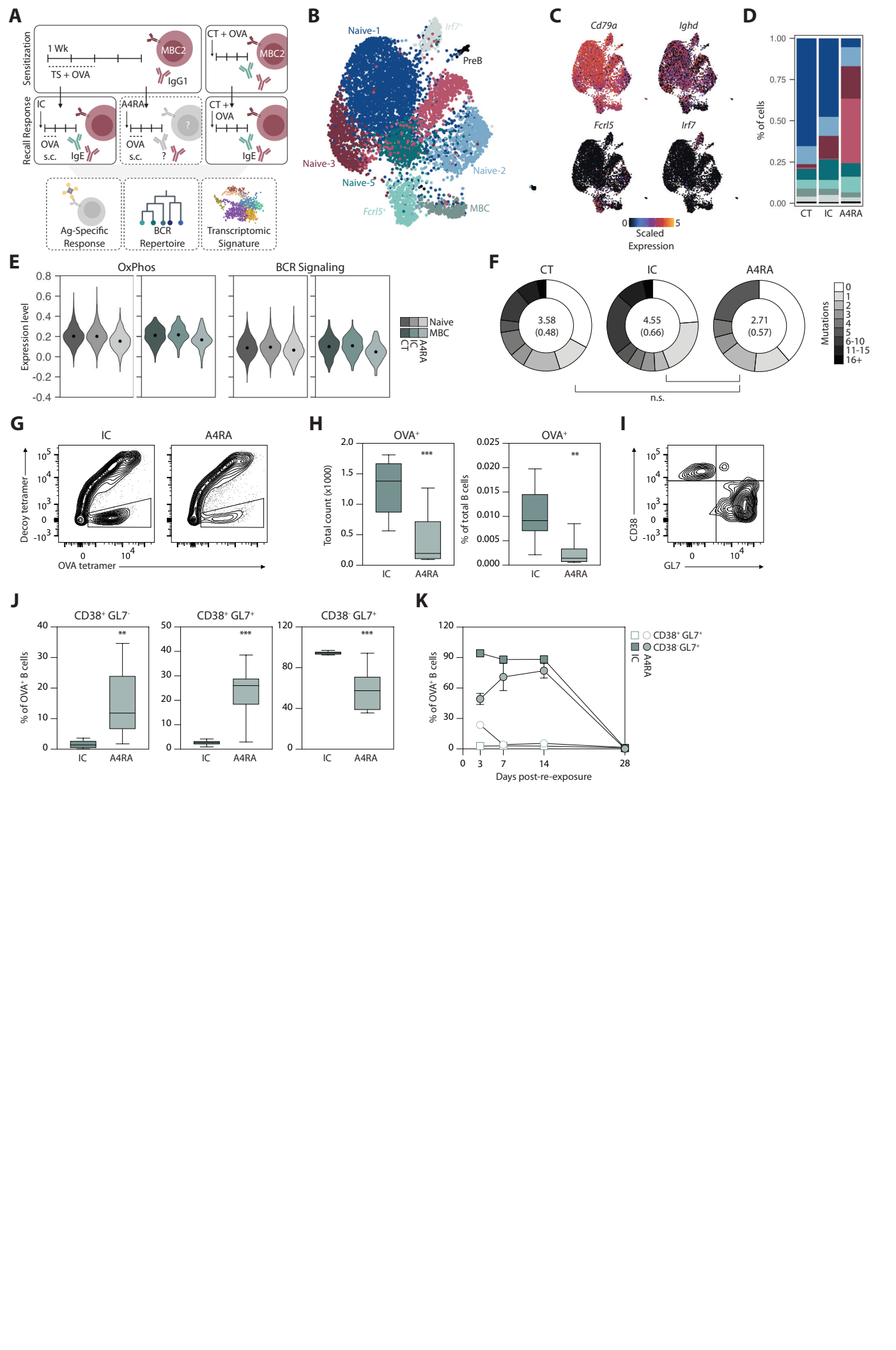
A
Sensitization
1 Wk
TS + OVA
MBC2
IgG1
CT + OVA
MBC2
Recall Response
IC
OVA
s.c.
IgE
A4RA
OVA
s.c.
?
CT +
OVA
IgE
Ag-Specific
Response
BCR
Repertoire
Transcriptomic
Signature
B
Naive-1
Irf7+
PreB
Naive-3
Naive-5
Naive-2
Fcrl5+
MBC
C
Cd79a
Ighd
Fcrl5
Irf7
0
5
Scaled
Expression
D
% of cells
1.00
0.75
0.50
0.25
0.00
CT
IC
A4RA
E
OxPhos
BCR Signaling
Expression level
0.8
0.6
0.4
0.2
0.0
-0.2
-0.4
Naive
MBC
IC
CT
A4RA
F
CT
IC
A4RA
3.58
(0.48)
4.55
(0.66)
2.71
(0.57)
Mutations
0
1
2
3
4
5
6-10
11-15
16+
n.s.
G
IC
A4RA
Decoy tetramer
OVA tetramer
H
OVA+
Total count (x1000)
***
IC
A4RA
OVA+
% of total B cells
**
IC
A4RA
I
CD38
GL7
J
CD38+ GL7-
% of OVA+ B cells
**
IC
A4RA
CD38+ GL7+
***
IC
A4RA
CD38- GL7+
***
IC
A4RA
K
% of OVA+ B cells
CD38+ GL7+
CD38- GL7+
IC
A4RA
0
3
7
14
28
Days post-re-exposure

Fig. 1. **IL-4Ra signaling augments secondary germinal center activity. (A)** Study schematic. **(B)** UMAP of B cell clusters from scRNA-seq analysis of B cells isolated from spleens and inguinal LNs of OVA-sensitized mice. Mice were either sensitized subcutaneously with CT or epicutaneously by tape-stripping. Epicutaneously sensitized mice were treated with either IC or A4RA prior to s.c. re-exposures and tissue harvest. $n = 5$ CT, $n = 10$ IC, $n = 10$ A4RA. **(C)** UMAP plots of genes defining naïve and MBC clusters. **(D)** Percent of cells in each cluster by treatment group. **(E)** Expression level of gene modules in naïve B cell clusters 1-5 (grey) and MBCs (green) by treatment group. Point indicates median. **(F)** VDJ analysis of MBCs identifying the number of nucleotide mutations compared to the germline sequence. Shading in circle plots depict the fraction of cells with each number of mutations. Mean (SEM) number of mutations are displayed within the circles. **(G)** Representative contour plots of enriched OVA^+ B cell population from inguinal LNs of epicutaneously sensitized mice. Pre-gated as live > singlet > $F4/80^-$ $CD3^-$ > $B220^+$. **(H)** Summary plots of OVA^+ B cell total count and frequency. **(I)** Representative contour plot of resting ($CD38^+$ $GL7^-$), transitional ($CD38^+$ $GL7^+$) and GC ($CD38^-$ $GL7^+$) B cells. Pre-gated from OVA^+ B cells > IgM^- IgD^-. **(J)** Summary plots of OVA^+ B cell frequency within the populations from (I) at three days post-boost. **(K)** Summary plot of OVA^+ B cell frequency within transitional (empty) and GC (filled) populations in post-boost time course. Data represent 2 experiments, each with 4 mice per group. Data are presented as median ± min/max (H, J) or mean ± SEM (K). ** $p < 0.01$, *** $p < 0.001$.

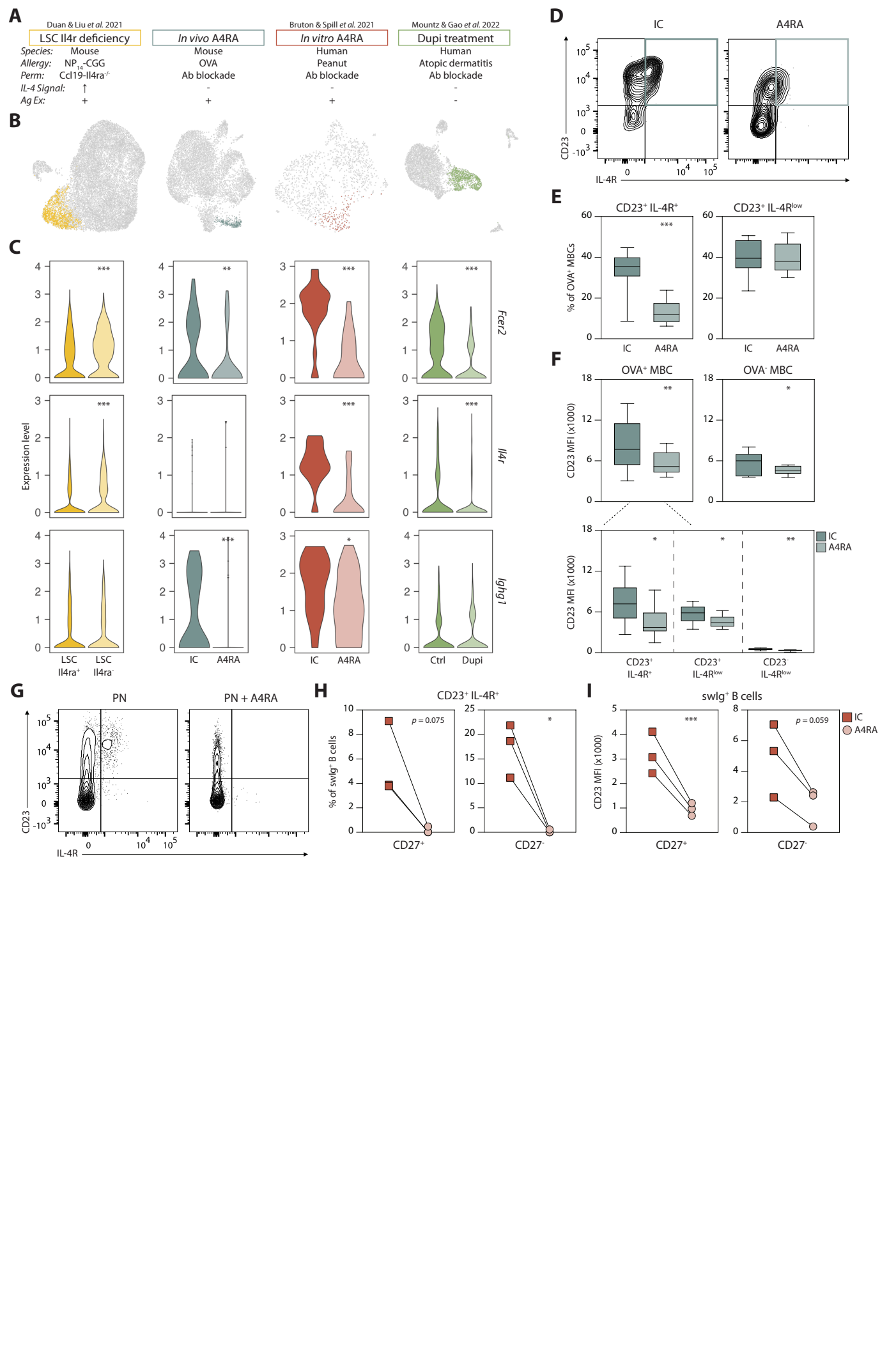
A
Duan & Liu et al. 2021
LSC Il4r deficiency
Species: Mouse
Allergy: NP14-CGG
Perm: Ccl19-Il4ra-/-
IL-4 Signal: ↑
Ag Ex: +
In vivo A4RA
Mouse
OVA
Ab blockade
-
+
Bruton & Spill et al. 2021
In vitro A4RA
Human
Peanut
Ab blockade
-
+
Mountz & Gao et al. 2022
Dupi treatment
Human
Atopic dermatitis
Ab blockade
-
-
B
C
Expression level
Fcer2
Il4r
Ighg1
LSC Il4ra+
LSC Il4ra-
IC
A4RA
Ctrl
Dupi
D
IC
A4RA
CD23
IL-4R
E
CD23+ IL-4R+
CD23+ IL-4Rlow
% of OVA+ MBCs
F
OVA+ MBC
OVA- MBC
CD23 MFI (x1000)
CD23+ IL-4R+
CD23+ IL-4Rlow
CD23- IL-4Rlow
G
PN
PN + A4RA
CD23
IL-4R
H
CD23+ IL-4R+
% of swIg+ B cells
p = 0.075
CD27+
CD27-
I
swIg+ B cells
CD23 MFI (x1000)
p = 0.059
CD27+
CD27-

Fig. 2. MBC2 phenotype is ameliorated with IL-4Ra blockade in mice and humans. (A) Overview of analyzed datasets. **(B)** UMAP of B cell clusters from scRNA-seq datasets. Colored points indicate class-switched cluster used for downstream analyses. **(C)** Expression level of MBC2-related genes in MBC clusters. **(D)** Representative contour plots of OVA^+ MBC2s from inguinal LNs of epicutaneously sensitized mice four weeks after re-exposure and Ab treatment. Pre-gated as OVA^+ B cells > $CD38^+$ $GL7^-$ > IgM^- IgD^-. **(E)** Summary plots of MBC2 and $CD23^+$ IL-$4R^{low}$ MBC frequency from IC and A4RA-treated epicutaneously sensitized mice. **(F)** MFI of CD23 within OVA^+ (top left) and OVA^- (top right) MBCs from IC and A4RA-treated epicutaneously sensitized mice and faceted by IL-4R and CD23 expression (bottom) within OVA^+ population. Pre-gated as $OVA^{+/-}$ B cells > $CD38^+$ $GL7^-$ > IgM^- IgD^-. **(G)** Representative contour plots of MBC2s from human PBMCs 8 days following *in vitro* allergen stimulation and treatment with IC or A4RA. Pre-gated as live > singlet > $CD3^-$ $CD14^-$ $CD16^-$ $CD19^+$ > IgD^- IgM^- > $CD38^{low-med}$. **(H)** Summary plots of human MBC2 frequency in **G**, separated by CD27 expression. **(I)** MFI of CD23 within $CD27^{+/-}$ class-switched B cells from human PBMCs 8 days following *in vitro* allergen stimulation and treatment with IC or A4RA. Data represent 2-3 experiments with 5 mice per group and are presented as median ± min/max (E, F) or 2 experiments (n = 3 blood donors) with each line representing a single donor (H, I). * $p < 0.05$, ** $p < 0.01$, *** $p < 0.001$. LSC, lymphoid stromal cell; Perm, permutation; Re-Ex, re-exposure.

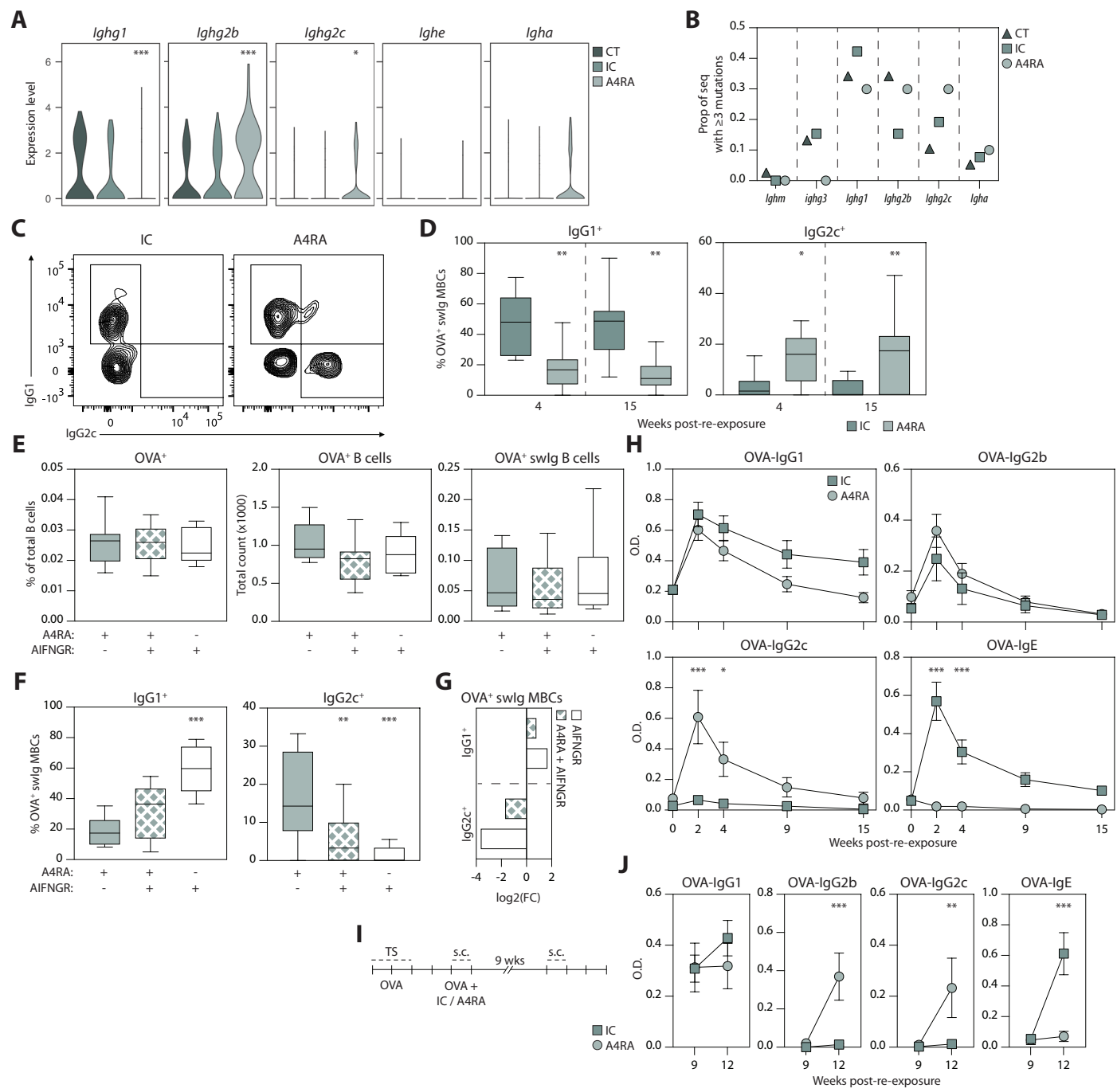
A
Ighg1
Ighg2b
Ighg2c
Ighe
Igha
Expression level
CT
IC
A4RA
B
Prop of seq with ≥3 mutations
Ighm
Ighg3
Ighg1
Ighg2b
Ighg2c
Igha
C
IC
A4RA
IgG1
IgG2c
D
IgG1+
IgG2c+
% OVA+ swIg MBCs
Weeks post-re-exposure
E
OVA+
OVA+ B cells
OVA+ swIg B cells
% of total B cells
Total count (x1000)
A4RA:
AIFNGR:
F
IgG1+
IgG2c+
% OVA+ swIg MBCs
G
OVA+ swIg MBCs
AIFNGR
A4RA + AIFNGR
log2(FC)
H
OVA-IgG1
OVA-IgG2b
OVA-IgG2c
OVA-IgE
O.D.
Weeks post-re-exposure
I
TS
s.c.
9 wks
s.c.
OVA
OVA + IC / A4RA
J
OVA-IgG1
OVA-IgG2b
OVA-IgG2c
OVA-IgE
O.D.
Weeks post-re-exposure

Fig. 3. Longitudinal analysis of Ag-specific B cell responses with absent IL-4 signaling. (A) Expression level of *Ighc* genes inclusive and downstream of *Ighg1* from scRNA-seq analysis of B cells isolated from spleens and inguinal LNs of CT-immunized mice and A4RA/IC-treated epicutaneously sensitized mice. Gene expression is plotted for cells within the MBC cluster (Fig. 1B). **(B)** VDJ analysis of MBC cluster. Plot depicts the assigned *Ighc* gene in MBCs with ≥3 nucleotide mutations compared to the germline sequence. **(C)** Representative contour plots of $IgG1^+$ and $IgG2c^+$ populations from inguinal LNs of IC/A4RA-treated epicutaneously sensitized mice four weeks post-boost and Ab treatment. **(D)** IC/A4RA-treated mice were rested up to 15 weeks after re-exposures. $IgG1^+$ (left) and $IgG2c^+$ (right) MBC frequency are plotted at four and 15 weeks post-boost. Pre-gated as OVA^+ B cells > $CD38^+$ $GL7^-$ > IgM^- IgD^-. **(E)** Epicutaneously sensitized mice were treated with A4RA, AIFNGR, or both at the time of subcutaneous re-exposure. Summary plots of OVA^+ B cell and swIg OVA^+ B cell total count and proportion of total B cells. **(F)** $IgG1^+$ (left) and $IgG2c^+$ (right) MBC frequency are plotted at four weeks post-boost. Pre-gated as OVA^+ B cells > $CD38^+$ $GL7^-$ > IgM^- IgD^-. **(H)** OVA-specific serum Ig profiles of IC/A4RA-treated mice at zero to 15 weeks post-boost. **(I)** IC/A4RA-treated mice were rested for nine weeks to allow for clearance of OVA-specific IgG2c and clearance of IC/A4RA blocking antibodies. Subsequently, mice received tertiary OVA exposures and serum was collected at week 12. **(J)** OVA-specific serum Ig profiles are depicted before and after tertiary exposures. (C-J) Data represent 2 experiments with at least 4 mice per group. Data are presented as mean ± SEM (H, J), median ± min/max (D-F), and mean (G). * $p < 0.05$, ** $p < 0.01$, *** $p < 0.001$. Seq, sequences; swIg, class-switched; AIFNGR, anti-IFN-gR1; OD, optical density; Wks, weeks.

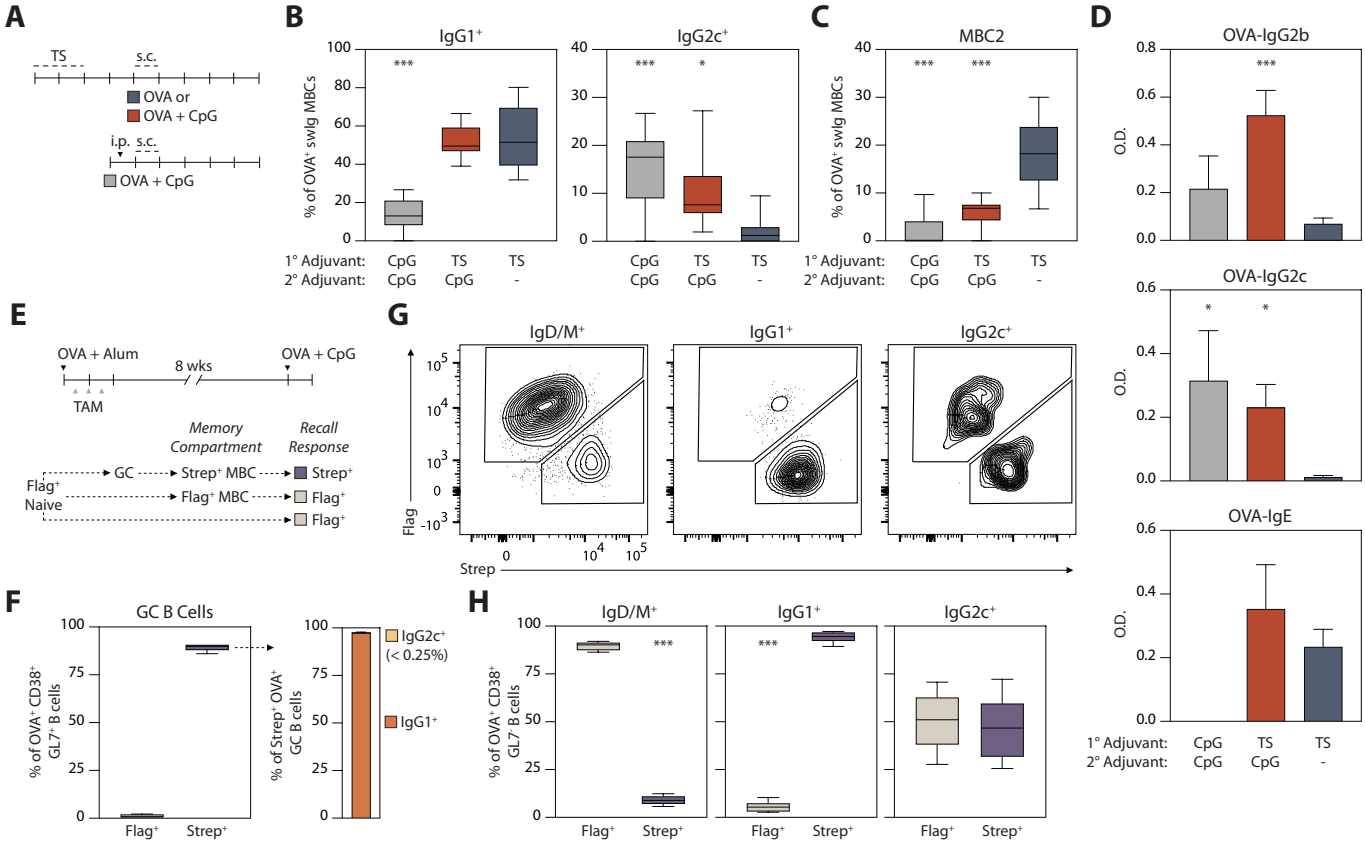
A
TS
s.c.
OVA or
OVA + CpG
i.p. s.c.
OVA + CpG
B
IgG1+
IgG2c+
% of OVA+ swIg MBCs
1° Adjuvant: CpG TS TS
2° Adjuvant: CpG CpG -
C
MBC2
% of OVA+ swIg MBCs
1° Adjuvant: CpG TS TS
2° Adjuvant: CpG CpG -
D
OVA-IgG2b
OVA-IgG2c
OVA-IgE
O.D.
1° Adjuvant: CpG TS TS
2° Adjuvant: CpG CpG -
E
OVA + Alum
8 wks
OVA + CpG
TAM
Memory Compartment
Recall Response
Flag+
Naive
GC
Strep+ MBC
Flag+ MBC
Strep+
Flag+
Flag+
G
IgD/M+
IgG1+
IgG2c+
Flag
Strep
F
GC B Cells
% of OVA+ CD38+ GL7+ B cells
Flag+
Strep+
% of Strep+ OVA+ GC B cells
IgG2c+ (< 0.25%)
IgG1+
H
IgD/M+
IgG1+
IgG2c+
% of OVA+ CD38+ GL7+ B cells
Flag+
Strep+

Fig 4. Boosting with type 1 adjuvant reprograms the type 2-primed response. (A) Experimental schematic. **(B,C)** IgG1$^+$ (left) and IgG2c$^+$ (right) MBC frequency (B) and MBC2 cell frequency (C) are plotted at four weeks post-secondary exposures with OVA alone or OVA + CpG. Pre-gated as OVA$^+$ B cells > CD38$^+$ GL7$^-$ > IgM$^-$ IgD$^-$. **(D)** OVA-specific serum Ig profiles. **(E)** Experimental schematic utilizing *S1pr2-Igk^{Tag}* mice. **(F)** Summary plots of Flag/Strep expression in OVA$^+$ CD38$^-$ GL7$^+$ B cells at 7 days post-TAM treatment (left) and IgG1/IgG2c expression in the Strep$^+$ population (right). **(G)** Representative contour plots of Flag/Strep expression in OVA$^+$ CD38$^+$ GL7$^-$ B cells from inguinal LNs one week after the recall response with OVA + CpG. **(H)** Summary plots of Flag/Strep expression in IgD/M$^+$ (left), IgG1$^+$ (middle), and IgG2c$^+$ (right) populations. Pre-gated as OVA$^+$ B cells > CD38$^+$ GL7$^-$. Data represent 2 experiments with at least 4 mice per group. Data are presented as mean ± SEM (D) or median ± min/max (B, C, F and H). * $p < 0.05$, ** $p < 0.01$, *** $p < 0.001$. OD, optical density; TAM, tamoxifen; Wks, weeks.

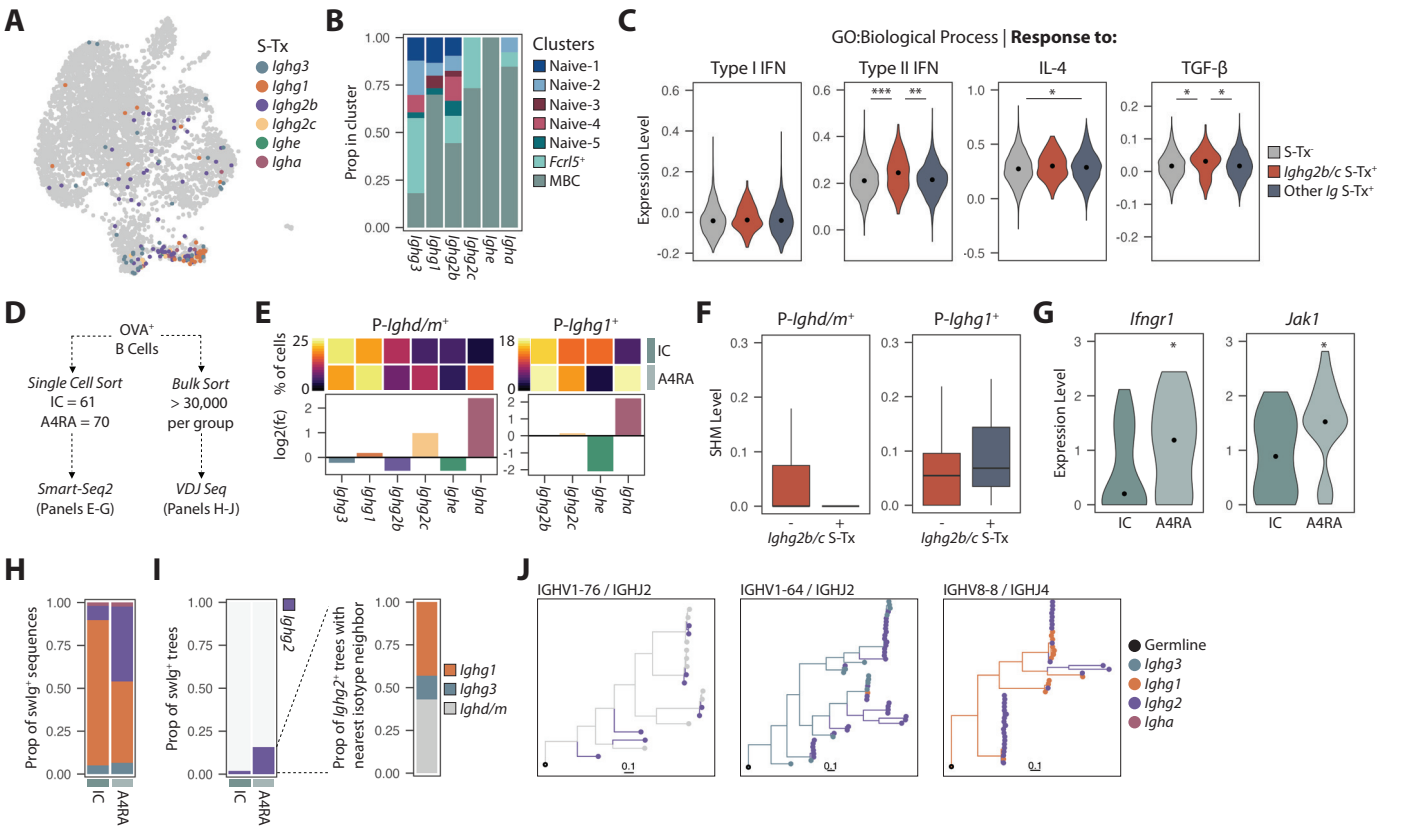
A
S-Tx
Ighg3
Ighg1
Ighg2b
Ighg2c
Ighe
Igha
B
Clusters
Naive-1
Naive-2
Naive-3
Naive-4
Naive-5
Fcrl5+
MBC
Prop in cluster
C
GO:Biological Process | Response to:
Type I IFN
Type II IFN
IL-4
TGF-β
Expression Level
S-Tx-
Ighg2b/c S-Tx+
Other Ig S-Tx+
D
OVA+ B Cells
Single Cell Sort
IC = 61
A4RA = 70
Bulk Sort
> 30,000
per group
Smart-Seq2
(Panels E-G)
VDJ Seq
(Panels H-J)
E
P-Ighd/m+
P-Ighg1+
% of cells
log2(fc)
IC
A4RA
F
P-Ighd/m+
P-Ighg1+
SHM Level
Ighg2b/c S-Tx
G
Ifngr1
Jak1
Expression Level
IC
A4RA
H
Prop of swIg+ sequences
I
Prop of swIg+ trees
Ighg2
Prop of Ighg2+ trees with nearest isotype neighbor
Ighg1
Ighg3
Ighd/m
J
IGHV1-76 / IGHJ2
IGHV1-64 / IGHJ2
IGHV8-8 / IGHJ4
Germline
Ighg3
Ighg1
Ighg2
Igha

Fig. 5. Clonal analysis of polyclonal and OVA-specific B cells. (A) UMAP of B cell clusters from scRNA-seq (Fig. 1B). Colored points indicate the most downstream *Igh* S-Tx expressed by a cell. **(B)** Distribution of S-Tx amongst B cell clusters. **(C)** Expression level of gene modules in B cells without S-Tx (grey), B cells with *Ighg2b/c* S-Tx (red), and B cells with other S-Tx (blue). Point indicates median. **(D)** Schematic depicting use of OVA-specific B cells for Smart-Seq2 and bulk VDJ sequencing experiments. **(E)** Heatmap displaying the percent of B cells expressing S-Tx downstream to their productive isotype and barplots depicting the fold change in S-Tx (IgD/M, left; IgG1, right) with A4RA treatment compared to IC. **(F)** SHM frequency between *Ighg2b/c* S-Tx^+ (red) and *Ighg2b/c* S-Tx^- (blue) B cells with productive IgD/M (left) or productive IgG1 (right). Data are presented as median ± min/max. **(G)** Expression level of genes from Smart-Seq2 analysis. Gene expression is plotted for cells with a productive *Ighg1* call from MBC clusters (n=22 cells per group). **(H)** Isotype usage amongst swIg sequences. **(I)** Proportion of clonal lineage trees containing *Ighg2* amongst trees with ≥ 2 isotypes (left) and nearest isotype neighbor amongst *Ighg2*-containing trees (right). **(J)** Representative clonal lineage trees containing *Ighg2* sequences and upstream isotypes (*Ighd/m*, *Ighg3*, and *Ighg1*) from A4RA-treated mice. Scale indicates IGHV SHM frequency. * $p < 0.05$, ** $p < 0.01$, *** $p < 0.001$. P, productive; Prop, proportion.

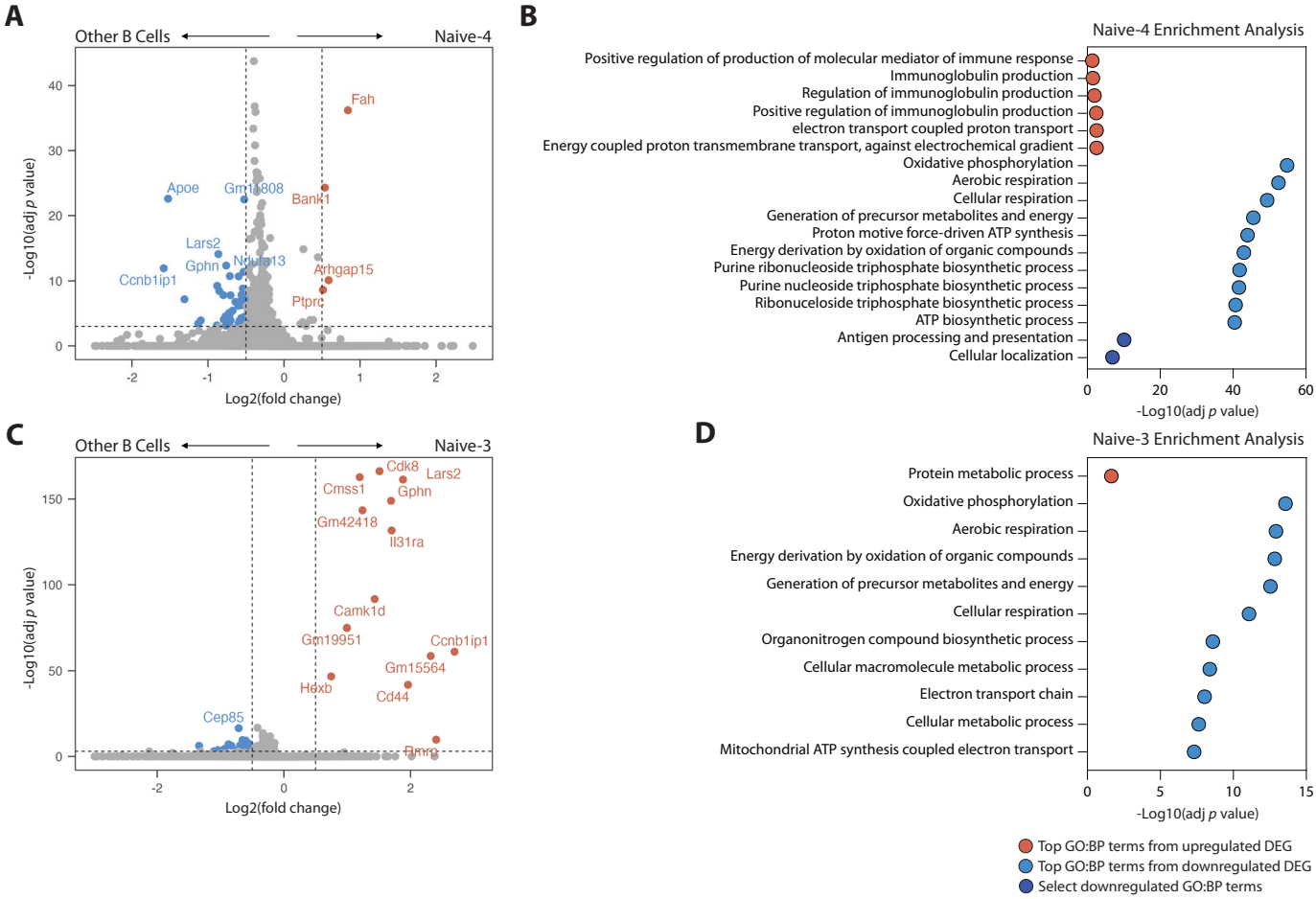
A
Other B Cells
Naive-4
Fah
Apoe
Gm11808
Bank1
Lars2
Gphn
Ndufa13
Arhgap15
Ccnb1ip1
Ptprc
-Log10(adj p value)
Log2(fold change)
B
Naive-4 Enrichment Analysis
Positive regulation of production of molecular mediator of immune response
Immunoglobulin production
Regulation of immunoglobulin production
Positive regulation of immunoglobulin production
electron transport coupled proton transport
Energy coupled proton transmembrane transport, against electrochemical gradient
Oxidative phosphorylation
Aerobic respiration
Cellular respiration
Generation of precursor metabolites and energy
Proton motive force-driven ATP synthesis
Energy derivation by oxidation of organic compounds
Purine ribonucleoside triphosphate biosynthetic process
Purine nucleoside triphosphate biosynthetic process
Ribonucleoside triphosphate biosynthetic process
ATP biosynthetic process
Antigen processing and presentation
Cellular localization
-Log10(adj p value)
C
Other B Cells
Naive-3
Cdk8
Lars2
Cmss1
Gphn
Gm42418
Il31ra
Camk1d
Gm19951
Ccnb1ip1
Gm15564
Hexb
Cd44
Cep85
Ptprc
-Log10(adj p value)
Log2(fold change)
D
Naive-3 Enrichment Analysis
Protein metabolic process
Oxidative phosphorylation
Aerobic respiration
Energy derivation by oxidation of organic compounds
Generation of precursor metabolites and energy
Cellular respiration
Organonitrogen compound biosynthetic process
Cellular macromolecule metabolic process
Electron transport chain
Cellular metabolic process
Mitochondrial ATP synthesis coupled electron transport
-Log10(adj p value)
Top GO:BP terms from upregulated DEG
Top GO:BP terms from downregulated DEG
Select downregulated GO:BP terms

Fig. S1. **Gene expression profiles of naïve B cell clusters. (A)** Volcano plot of differentially expressed genes in Naïve-4 (A) and Naïve-3 (C) clusters. Red points indicate genes with -log10 adjusted *p* value > 5 and log2 fold change ± 0.5. **(B, D)** GO:BP enrichment analysis of significantly upregulated (red) and downregulated (blue) genes, excluding ribosomal genes, in Naïve-4 (B) and Naïve-3 (D) clusters. DEG, differentially expressed genes.

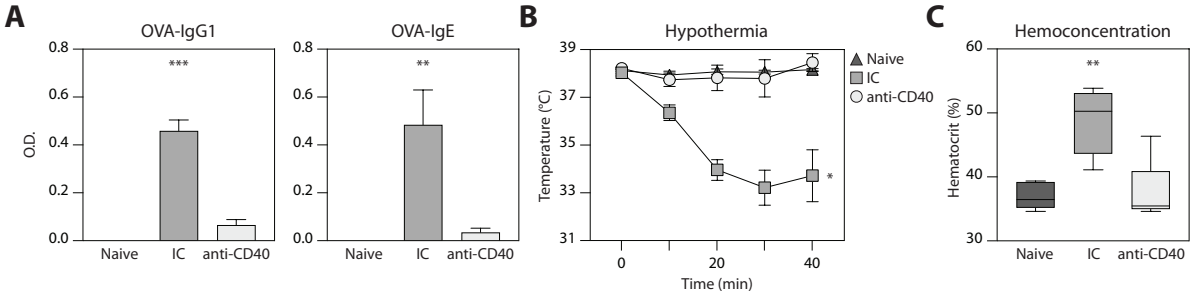
A
OVA-IgG1
OVA-IgE
O.D.
0.8
0.6
0.4
0.2
0.0
***
**
Naive
IC
anti-CD40
B
Hypothermia
Temperature (ºC)
39
37
35
33
31
0
20
40
Time (min)
*
Naive
IC
anti-CD40
C
Hemoconcentration
Hematocrit (%)
60
50
40
30
**
Naive
IC
anti-CD40

Fig. S2. Requirement of B-T interactions for IgE recall responses. (A) Serum OVA-specific immunoglobulins immediately prior to allergen challenge. **(B)** Core body temperature. **(C)** Hemoconcentration measured 40-minutes post-allergen challenge. Data represent 2 experiments, each with 4 mice per group. Data are presented as mean ± SEM (A, B) or median ± min/max (C). * $p < 0.05$, ** $p < 0.01$, *** $p < 0.001$.

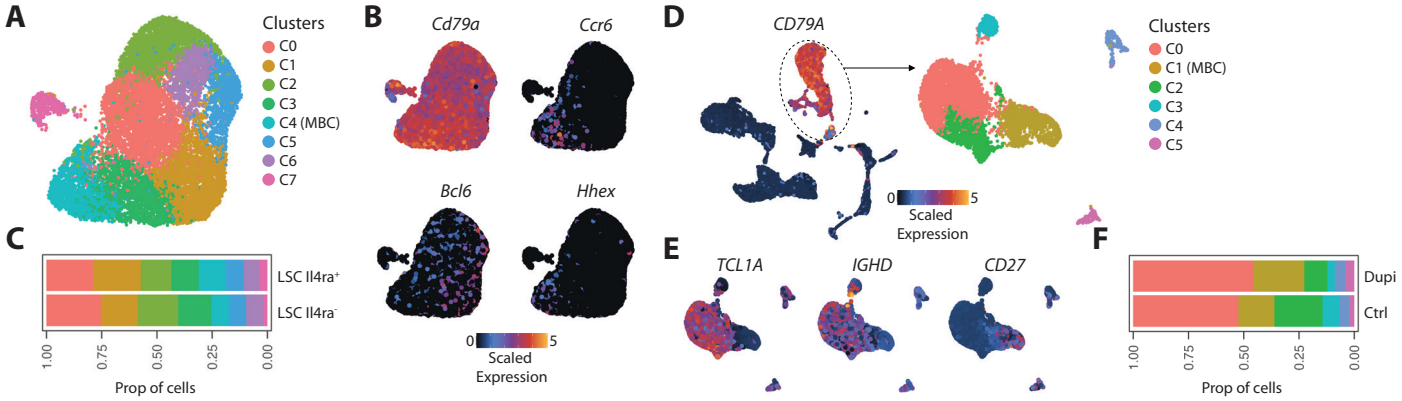
A
Clusters
C0
C1
C2
C3
C4 (MBC)
C5
C6
C7
B
Cd79a
Ccr6
Bcl6
Hhex
0
5
Scaled
Expression
C
LSC Il4ra+
LSC Il4ra-
1.00
0.75
0.50
0.25
0.00
Prop of cells
D
CD79A
0
5
Scaled
Expression
Clusters
C0
C1 (MBC)
C2
C3
C4
C5
E
TCL1A
IGHD
CD27
F
Dupi
Ctrl
1.00
0.75
0.50
0.25
0.00
Prop of cells

Fig. S3. Analysis of publicly reposited scRNA-seq datasets. (A, D) UMAP of B cell clusters from scRNA-seq analysis of Duan & Liu *et al.* (2021) (A) and Mountz & Gao *et al.* (2022) (D) datasets. **(B, E)** UMAP plots of scaled gene expression used to define MBC clusters. **(C, F)** Percent of cells in each cluster. LSC, lymphoid stromal cell.

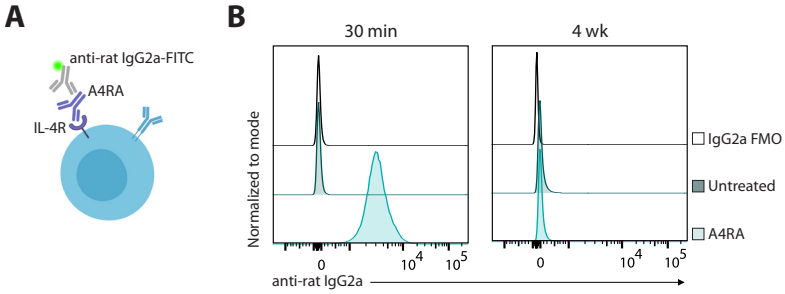
A
anti-rat IgG2a-FITC
A4RA
IL-4R
B
30 min
4 wk
Normalized to mode
IgG2a FMO
Untreated
A4RA
0
10^4
10^5
anti-rat IgG2a

Fig. S4. Surface expression of A4RA blocking antibody. (A) A4RA-treated cells were stained with an anti-rat IgG2a-FITC antibody to detect the Fc region of A4RA. **(B)** Representative histograms of surface rat-IgG2a expression in mouse B cells four weeks after *in vivo* A4RA administration (right). As a comparison, splenocytes from untreated mice were incubated with A4RA for 30 minutes prior to staining with fluorochrome conjugated antibodies (left). FMO, fluorescence minus one.

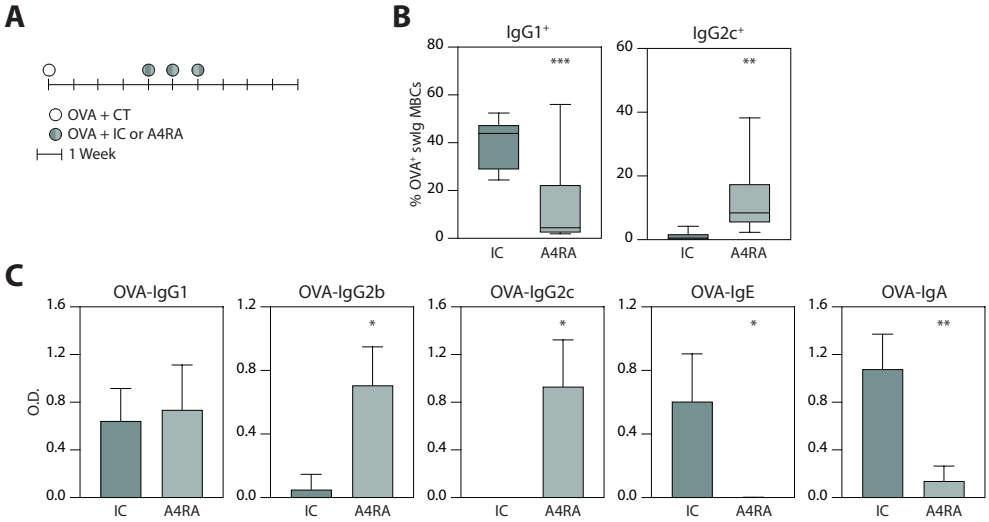
A
OVA + CT
OVA + IC or A4RA
1 Week
B
IgG1+
IgG2c+
% OVA+ swIg MBCs
80
60
40
20
0
***
**
IC
A4RA
C
OVA-IgG1
OVA-IgG2b
OVA-IgG2c
OVA-IgE
OVA-IgA
O.D.
1.6
1.2
0.8
0.4
0.0
*
**

Fig. S5. B cell reprogramming in orally-sensitized mice. (A) Experimental schematic. **(B)** Summary plots of IgG1+ (left) and IgG2c+ (right) MBC frequency oral re-exposures. **(C)** OVA-specific serum immunoglobulin profiles post-boost. Data represent 2 experiments, each with 4 mice per group. Data are presented as median ± min/max (B) or mean ± SEM (C). * $p < 0.05$, ** $p < 0.01$, *** $p < 0.001$.

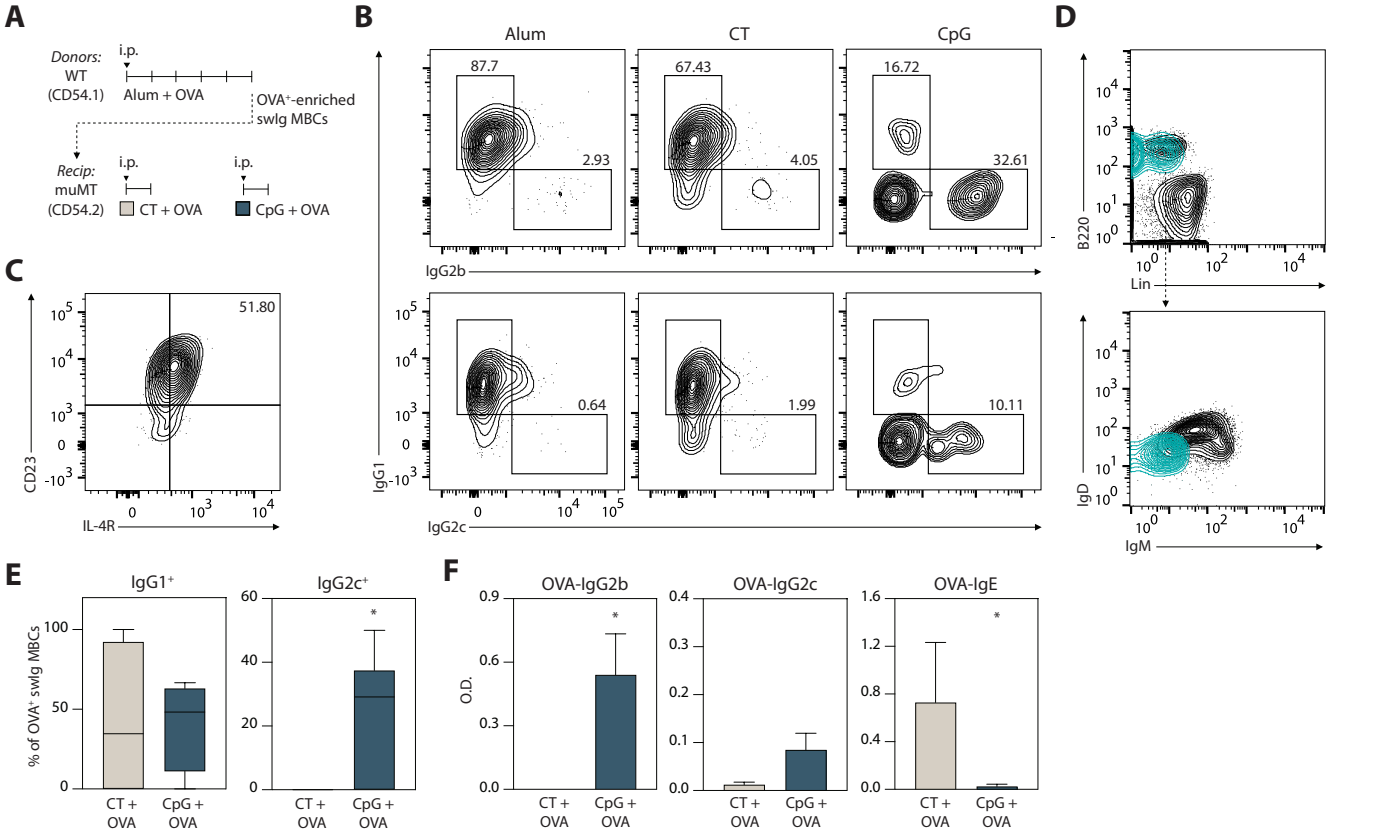
A
Donors:
WT
(CD54.1)
i.p.
Alum + OVA
OVA+-enriched
swIg MBCs
Recip:
muMT
(CD54.2)
i.p.
CT + OVA
i.p.
CpG + OVA
B
Alum
CT
CpG
87.7
2.93
67.43
4.05
16.72
32.61
IgG2b
0.64
1.99
10.11
IgG1
IgG2c
C
51.80
CD23
IL-4R
D
B220
Lin
IgD
IgM
E
IgG1+
IgG2c+
% of OVA+ swIg MBCs
CT + OVA
CpG + OVA
F
OVA-IgG2b
OVA-IgG2c
OVA-IgE
O.D.

Fig. S6. Boost with CpG produces IgG2 response from type 2-primed class-switched MBCs in adoptive transfer model. (A) Adoptive transfer schematic. **(B)** To illustrate the isotype distribution of class-switched MBCs, WT mice were immunized with OVA + Alum, CT, or CpG. Representative contour plots class-switched OVA+ MBCs. Pre-gated as OVA^+ B cells > $CD38^+$ $GL7^-$ > IgM^- IgD^-. Numbers indicate the proportion of $IgG1^+$, $IgG2b^+$, and $IgG2c^+$ cells from the parent class-switched MBC population. **(C)** Representative contour plot of CD23 and IL-4R expression from OVA^+ $IgG1^+$ MBCs in OVA + Alum-immunized mice. Number indicates the proportion of $CD23^+$ IL-$4R^{hi}$ cells from the parent OVA^+ $IgG1^+$ MBC population. **(D)** Contour plots depicting the adoptively transferred class-switched B cell population (blue) from OVA-enriched B cells of OVA + Alum-immunized mice. **(E)** Summary plots depicting donor (CD45.1+) OVA+ IgG1+ and OVA+ IgG2c+ B cell frequency in recipient mice one week post-transfer and boost. **(F)** OVA-specific serum immunoglobulin profiles in recipient mice one week post-transfer and boost. Data represent 2 experiments, each with 2-4 mice per group. Data are presented as median ± min/max (E) or mean ± SEM (D, F). * $p < 0.05$.

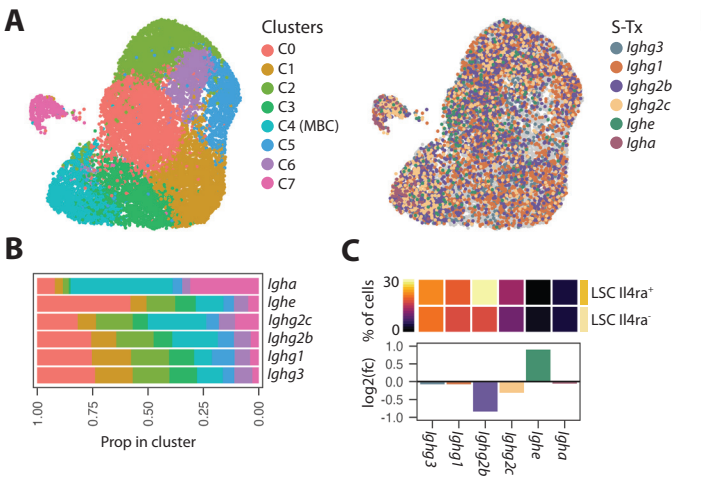
A
Clusters
C0
C1
C2
C3
C4 (MBC)
C5
C6
C7
S-Tx
Ighg3
Ighg1
Ighg2b
Ighg2c
Ighe
Igha
B
Igha
Ighe
Ighg2c
Ighg2b
Ighg1
Ighg3
1.00
0.75
0.50
0.25
0.00
Prop in cluster
C
% of cells
30
0
LSC Il4ra+
LSC Il4ra-
log2(fc)
1.0
0.5
0.0
-0.5
-1.0
Ighg3
Ighg1
Ighg2b
Ighg2c
Ighe
Igha
D
Ifngr1
***
Jak1
**
Expression level
2.5
2.0
1.5
1.0
0.5
0.0
LSC Il4ra+
LSC Il4ra-

Fig. S7. Ig S-Tx usage with increased IL-4 bioavailability in mice. **(A)** UMAP of B cell clusters from scRNA-seq analysis of Duan & Liu *et al.* (2021) and overlay of S-Tx expression (right). Colored points indicate the most downstream *Igh* S-Tx expressed by a cell. **(B)** Distribution of S-Tx amongst B cell clusters. **(C)** Heatmap displaying the percent of B cells expressing S-Tx downstream to their productive isotype and barplots depicting the fold change in S-Tx expression in LSC Il4ra^{-} compared to LSC Il4ra^{+}. **(D)** Expression level of genes in MBC cluster. ** $p < 0.01$, *** $p < 0.001$.

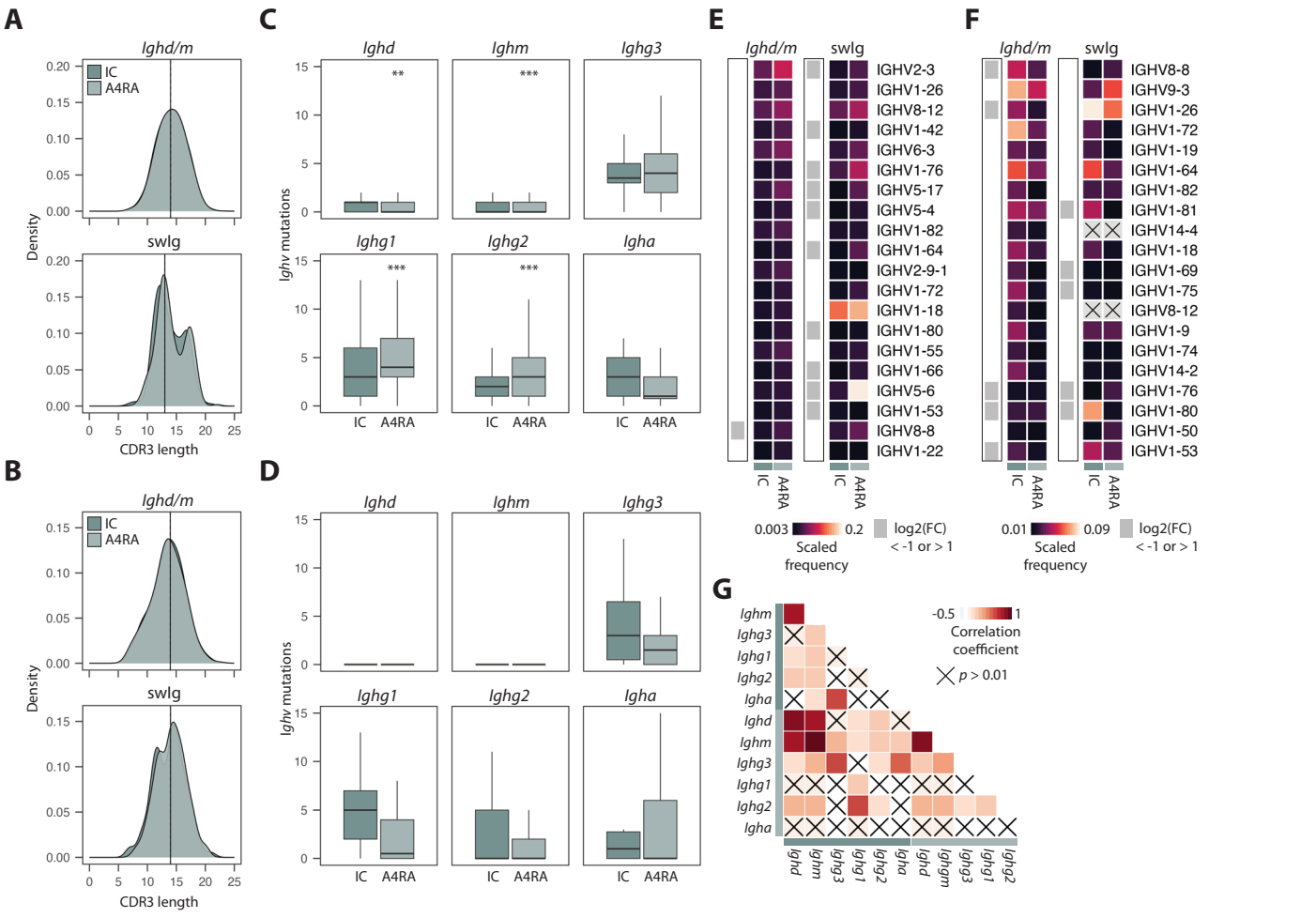
A
Ighd/m
IC
A4RA
Density
swIg
CDR3 length
B
C
Ighd
Ighm
Ighg3
Ighg1
Ighg2
Igha
Ighv mutations
IC
A4RA
D
E
F
IGHV2-3
IGHV1-26
IGHV8-12
IGHV1-42
IGHV6-3
IGHV1-76
IGHV5-17
IGHV5-4
IGHV1-82
IGHV1-64
IGHV2-9-1
IGHV1-72
IGHV1-18
IGHV1-80
IGHV1-55
IGHV1-66
IGHV5-6
IGHV1-53
IGHV8-8
IGHV1-22
IGHV8-8
IGHV9-3
IGHV1-26
IGHV1-72
IGHV1-19
IGHV1-64
IGHV1-82
IGHV1-81
IGHV14-4
IGHV1-18
IGHV1-69
IGHV1-75
IGHV8-12
IGHV1-9
IGHV1-74
IGHV14-2
IGHV1-76
IGHV1-80
IGHV1-50
IGHV1-53
0.003
0.2
Scaled frequency
log2(FC) < -1 or > 1
0.01
0.09
G
Ighm
Ighg3
Ighg1
Ighg2
Igha
Ighd
-0.5
1
Correlation coefficient
p > 0.01

Fig. S8. VDJ repertoire analysis in OVA-enriched bulk sequencing and 10X datasets. (A, B) Distribution of CDR3 amino acid length in OVA-specific B cells (A) and polyclonal B cells (B). Solid and dashed lines indicate median length for IC and A4RA, respectively. **(C, D)** SHM count in IGHV region of OVA-specific B cells (C) and polyclonal B cells (D) presented as median ± min/max. **(E, F)** Heatmap of scaled IGHV gene usage for top 20 used IGHV genes in OVA-specific B cells (E) and polyclonal B cells (F). Grey squares indicate IGHV genes with log2 fold change ± 1 between IC and A4RA. Crosses indicate IGHV genes that are not present in the swIg cluster. **(G)** Correlation matrix of paired IGHV-IGHJ gene usage between isotypes in IC and A4RA. ** $p < 0.01$, *** $p < 0.001$.